



**CEN/TC 264/WG 23 “Methods for determination of the velocity
and the volumetric flow in stationary source emissions”**

Summary report of Laboratory and Field Trials

Contents

1	INTRODUCTION	3
2	RELATED DOCUMENTS	3
3	BACKGROUND	3
4	METHODS AND EQUIPMENT	5
4.1	MANUAL METHODS	5
4.2	AUTOMATIC METHODS.....	8
5	LABORATORY TESTS	16
5.1	DESCRIPTION OF WIND TUNNELS	16
5.2	DESCRIPTION OF THE LAB TESTS.....	18
6	FIELD TESTS	20
6.1	COPENHAGEN (WASTE INCINERATOR).....	20
6.2	WILHELMSHAVEN (COAL FIRED POWER PLANT).....	21
7	ANALYSIS OF VALIDATION STUDIES	22
7.1	INTRODUCTION	22
7.2	OVERVIEW OF TECHNIQUES ASSESSED IN VALIDATION STUDIES.....	22
7.3	SUMMARY OF PERFORMANCE DATA FROM LABORATORY STUDIES.....	24
7.4	PERFORMANCE EVALUATION OF FIELD TEST 1 'COPENHAGEN'	26
7.5	PERFORMANCE EVALUATION OF FIELD TEST 2, 'WILHELMSHAVEN'	40
7.6	CONCLUSIONS	47

1 Introduction

The EC and EFTA have given a mandate (M/401) to CEN for the standardization of the determination of the velocity and the volumetric flow in stationary source emissions to enable comparability of measured values and to enable the calculation of emitted mass flows. Working Group CEN/TC 264/WG 23 is responsible for planning and performing laboratory tests as well as field tests to validate the method(s) to be standardized.

The tests are subdivided into two parts:

- Laboratory tests at a wind tunnel site with a series of test runs involving manual methods (SRM) and automatic measuring methods (AMS)
- Field tests at two plants site with a series of test runs involving manual methods (SRM) and automatic measuring methods (AMS)

This summary report describes an overview of the processes and statistical evaluation of the various trials. Full reports on the validation studies are available through the CEN TC264 Secretariat.

The laboratory trials were carried out at wind tunnels at Technische Universität Berlin, Institut für Luft- und Raumfahrt, (TUB). The fan of the wind tunnel was rented by TUB, the wind tunnel was manufactured and delivered by Müller-BBM (MBBM). Further testing was carried out on a heated wind tunnel at TUB.

The field trials were carried out at;

1. Waste Incinerator - Amagerforbrænding, Copenhagen, Denmark.
2. Coal fired power plant - E.ON Kraftwerke GmbH, Kraftwerk, Wilhelmshaven, Germany

2 Related documents

This summary report has been extracted from the following individual reports for laboratory, field tests and statistical evaluation.

1. CEN TC 264 WG23 N235 Final report of Muller lab tests M81522_04_BER_4D
CEN TC 264 WG23 N235a Additional Muller tests December 2010 M81522_05_Brf_1D
2. CEN TC 264 WG23 N236 Final Copenhagen field trial report
3. CEN TC 264 WG23 N237 Final Wilhelmshaven field trial report
4. CEN TC 264 WG23 N238 Validation Studies- data analysis

These documents provide more detailed descriptions and data from the validation studies than are presented in this summary report.

3 Background

Flue gas velocity measurement, and its derivative volumetric flow, is needed for testing compliance with both PM (particle matter) emission limit values and for all mass emission limits whether PM, pollutants entrained on PM, or gases. It may also be needed to establish installation specific emission factors used in emission inventories.

Mass emission is calculated from the gas concentrations multiplied by the volume of emitted gas. An emission factor is an indicator of mass emission as a function of activity rate. If measurement-derived data has been used its quality depends on the suitability of the measurement method used.

The representativeness of a data set relates to how well the emission population has been sampled. The most suitable measurement methods are those that have been developed by standards organisations and have been field-tested to determine their operational characteristics. European Standards (CEN) or suitable validated national standards (EPA, VDI, etc) meet these criteria. International Standards Organisation (ISO) standards may also have field validation but most do not.

A modernized flow measurement standard is highly desirable and urgently needed. and the performance criteria based standards developed by WG23 are intended for use to meet the requirements of:

- Directive 2000/76/EC on the limitation of emissions of certain pollutants into the air from incineration plants,
- Directive 2001/80/EC on the limitation of emissions of certain pollutants into the air from large combustion plants,
- Directive 96/61/EC concerning pollution, prevention and control (IPPC),

but may be used in other industries where, however, the standard is not validated by experimental work. Commission Decision 29/01/2004 establishing guidelines for the monitoring and reporting of greenhouse gas emissions pursuant to Directive 2003/87/EC proposes the use of a tiered approach to the quantification of CO₂ and encourages the use of measurement for the determination of emission factors¹). The standards are also intended to meet the requirements of the Industrial Emissions Directive.

Reference documents

The following documents were used in the definition and procedures for the laboratory and field tests.

1. Specification for validation measurements of methods for determination of the velocity and the volumetric flow in stationary source emissions (Mandate M/401)
2. EN 14 181: Stationary source emissions - Quality assurance of automated measuring systems; September 2004
3. ISO 5725-2: Accuracy (trueness and precision) of measurement methods and results –Part 2: Basic method of the determination of repeatability and reproducibility of standard measurement methods; December 2002
4. EN 15 259: Air quality – Measurement of stationary source emissions – Requirements for measurement sections and sites and for the measurement objective, plan and report; October 2007
5. Wolfgang Nitsche: Strömungsmesstechnik (flow measurements); Springer Verlag Heidelberg 2006
6. EPA: Method 2F—determination of stack gas velocity and volumetric flow rate with three-dimensional probes
7. ISO 20 988: Guidelines for estimating measurement uncertainty (ISO 20988:2007)
8. DIRECTIVE 2000/76/EC OF THE EUROPEAN PARLIAMENT AND OF THE COUNCIL of 4 December 2000 on the incineration of waste
9. DIRECTIVE 2001/80/EC OF THE EUROPEAN PARLIAMENT AND OF THE COUNCIL of 23 October 2001 on the limitation of emissions of certain pollutants into the air from large combustion plants

10. Council Directive 96/61/EC concerning integrated pollution prevention and control, IPPC
11. Directive 2003/87/EC of the European Parliament and of the Council of 13 October 2003 establishing a scheme for greenhouse gas emission allowance trading within the Community and amending Council Directive 96/61/EC
12. ISO 3966; Measurement of fluid flow in closed conduits - Velocity area method using Pitot static tubes; 7/2008;

4 Methods and equipment

The following method and related equipment was used in the laboratory and field tests.

4.1 Manual methods

4.1.1 L type Pitot

The L Pitot is a basic Pitot tube which consists of a tube pointing directly into the fluid flow. As this tube contains fluid, a pressure can be measured. The moving fluid is brought to rest (stagnates) as there is no outlet to allow flow to continue. This pressure is the stagnation pressure of the fluid, also known as the total pressure or (particularly in aviation) the Pitot pressure.

The following figure shows the measurement principal of the L Pitot tube.

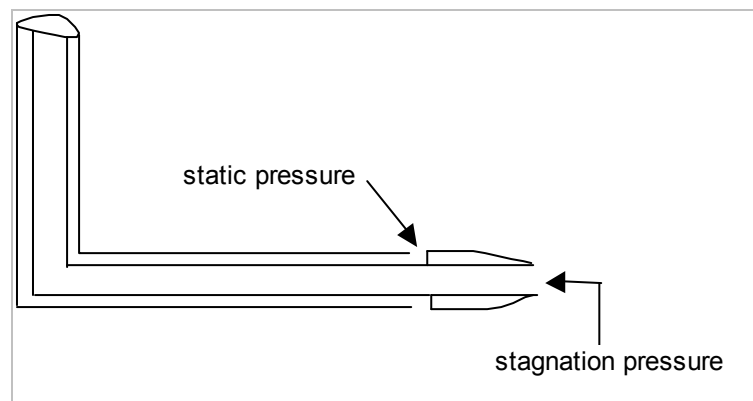


Figure 1 L type Pitot



Figure 2 Actual L type Pitot

The dynamic pressure is calculated based on the following equation:

$$p_{\text{dyn.}} = p_{\text{stag.}} - p_{\text{static}} \quad \text{eq. (1)}$$

where

$p_{\text{dyn.}}$: dynamic pressure
 $p_{\text{stag.}}$: stagnation pressure
 p_{static} : static pressure

The resulting velocity is:

$$v = \sqrt{\frac{2 * p_{\text{dyn.}}}{\rho(p, T)}} [m/s] \quad \text{eq. (2)}$$

Where

v : velocity [m/s]
 $\rho(p, T)$: density of fluid [kg/m³]

4.1.2 S type Pitot

The S type Pitot is also a basic Pitot tube which measures directly in the flow. The principle of work is similar to the L type Pitot. The velocity is calculated on the same way as for the L type Pitot. The S type Pitot has to be calibrated against a reference method because the measured “static” pressure is not the real static pressure. The velocity factor f_v is often expected to be approximately ~0,84 (see equation (3)).

$$v = f_v * \sqrt{\frac{2 * p_{\text{dyn.}}}{\rho(p, T)}} [m/s] \quad \text{eq. (3)}$$

Figure 3 shows the principal assembling of a S type Pitot, picture 4 shows the type of the S Pitot used in the validation tests.

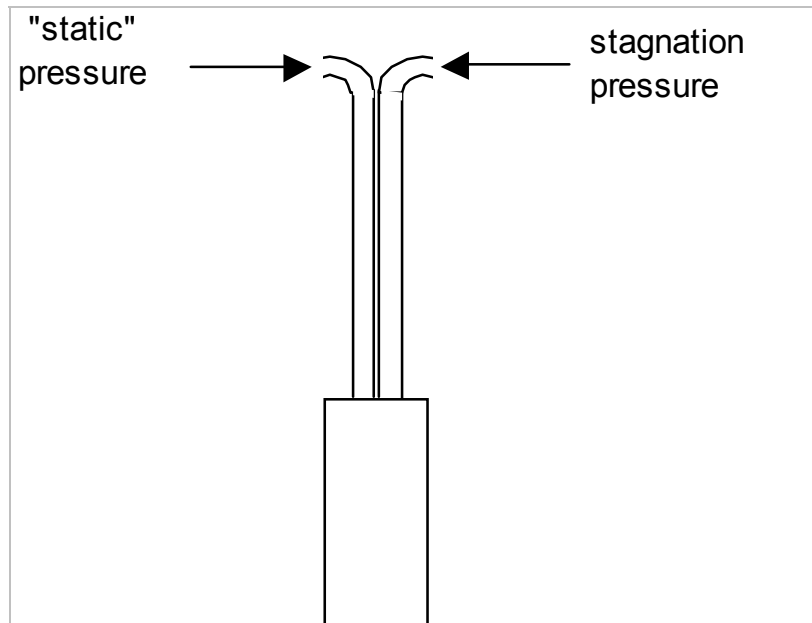


Figure 3 S Type Pitot

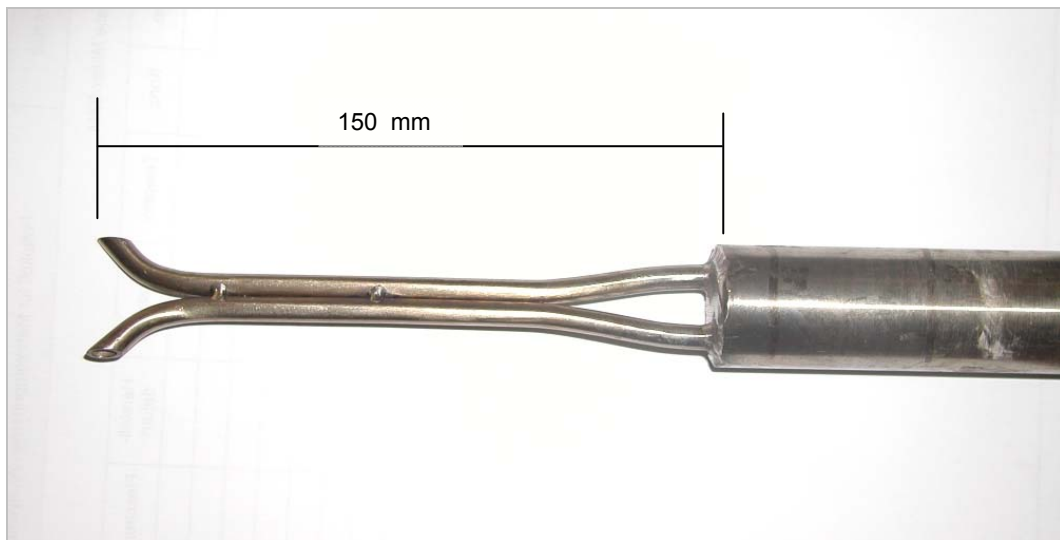


Figure 4 S type Pitot

4.1.3 3D type Pitot

This type of probe consists of five pressure taps in a spherical (or prism-shaped, which was not used on lab tests) sensing head. The pressure taps are numbered 1 through 5, with the pressures measured at each hole referred to as P1, P2, P3, P4, and P5, respectively.

The differential pressure P2-P3 is used to yaw null the probe and determine the yaw angle; the differential pressure P4-P5 is a function of pitch angle; and the differential pressure P1-P2 is a function of total velocity. In Figure 5 a typical spherical 3D Pitot is shown.

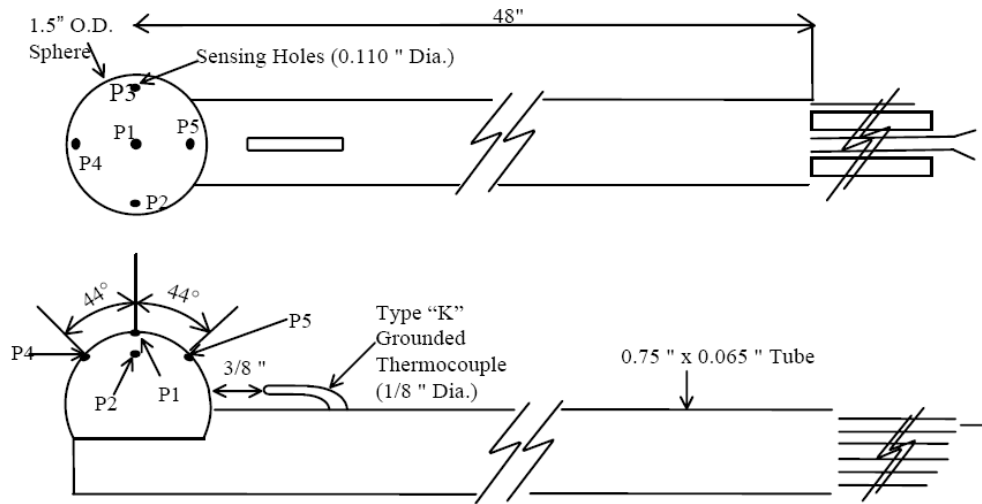


Figure 5 3D type Pitot

The procedures and equations describing how to calculate the velocity, the yaw, the pitch and the volumetric gas flow can be found in US EPA Method 2F.

4.2 Automatic methods

4.2.1 Ultrasonic measurement cross duct/ultrasonic single-probe version

The ultrasonic devices (FLOWSIC100) operate by measuring the transit time difference of ultrasonic pulses. Sender/receiver units are mounted on both sides of a duct/pipeline at a certain angle to the gas flow. These sender/receiver units contain piezoelectric ultrasonic transducers that function alternately as senders and receivers. The sound pulses are emitted at the angle α to the flow direction of the gas. Depending on the angle α and the gas velocity v , the transit time of the respective sound direction varies as a result of certain "acceleration and braking effects" (see formulas below). The difference in the transit times of the sound pulses increases, the higher the gas velocity and the smaller the angle to the flow direction is.

The gas velocity v is calculated from the difference between both transit times, independent of the sound velocity. Changes in the sound velocity caused by pressure or temperature fluctuations, therefore, do not affect the calculated gas velocity with this method of measurement. The flow velocity can be calculated as follows:

$$T_{AB} = \frac{L}{c + v * \cos \alpha} \quad \text{eq. (12)}$$

$$T_{BA} = \frac{L}{c - v * \cos \alpha} \quad \text{eq. (13)}$$

$$v[m/s] = \left(\frac{1}{T_{AB}} - \frac{1}{T_{BA}} \right) * \frac{L}{2 * \cos \alpha} \quad \text{eq. (14)}$$

Where

T_{BA} :	signal transit time in countercurrent with the direction of flow
T_{AB} :	signal transit time in the direction of flow
L :	measuring path = active measuring distance
α :	Angel of inclination
c :	speed of sound

In Figure 6 shows the cross duct measuring setup and Figure 7 shows the measuring setup for the point in-situ installation.

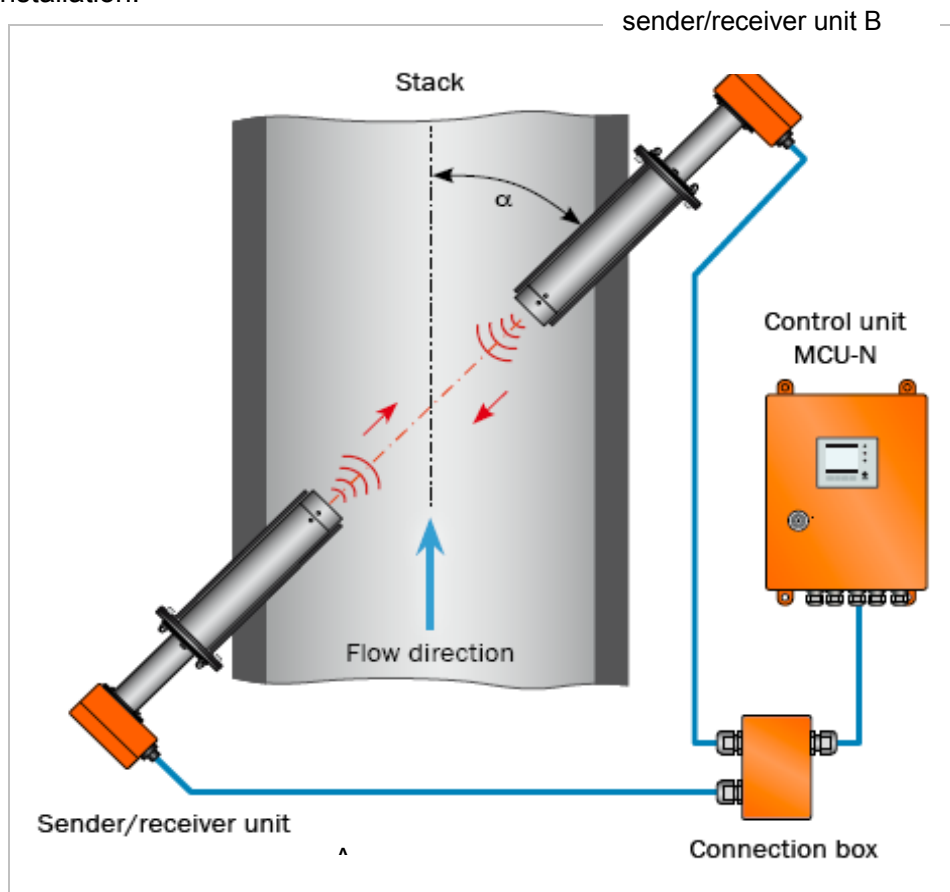


Figure 6 Cross duct ultrasonic transit time measurement (picture by Sick)

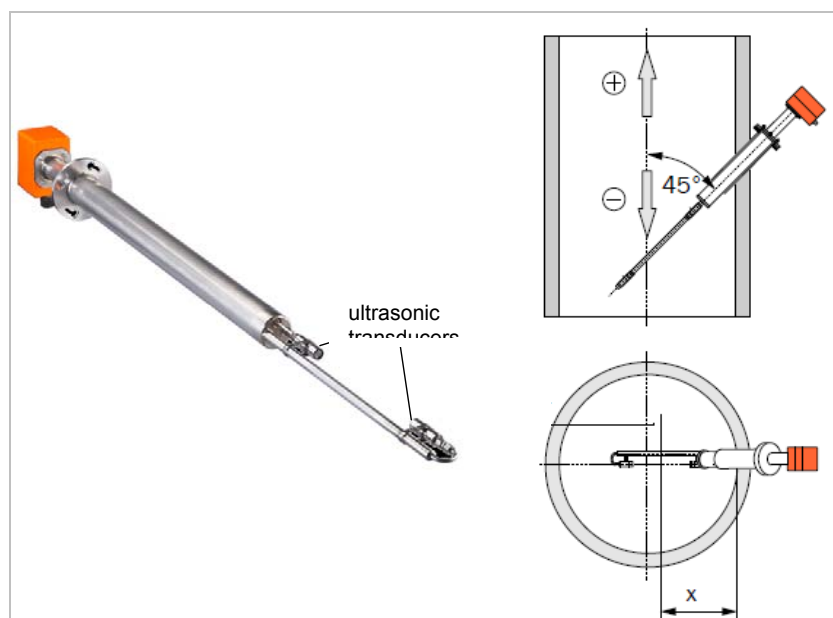


Figure 7 Single probe version ultrasonic transit time measurement (picture by Sick)

The single probe version contains 1 pc. of sender/receiver unit (single path configuration) containing 2 ultrasonic transducers with a fixed path length.

The sender/receiver unit is mounted on one side of a duct with a defined insertion depth in the gas flow (depending on duct size). The ultrasonic signal is transmitted on the measurement path between both transducer.

For multi path configurations the number of sender/receiver units is increased (2 pcs. installed parallel across the secants of the duct for 2-path measurement). In the field test programme cross duct installations were used in both the single and dual path configurations.

4.2.2 Differential pressure measurement

The differential pressure probe generates a signal proportional to the square of the flow rate. The differential pressure is measured as illustrated in Figure 8

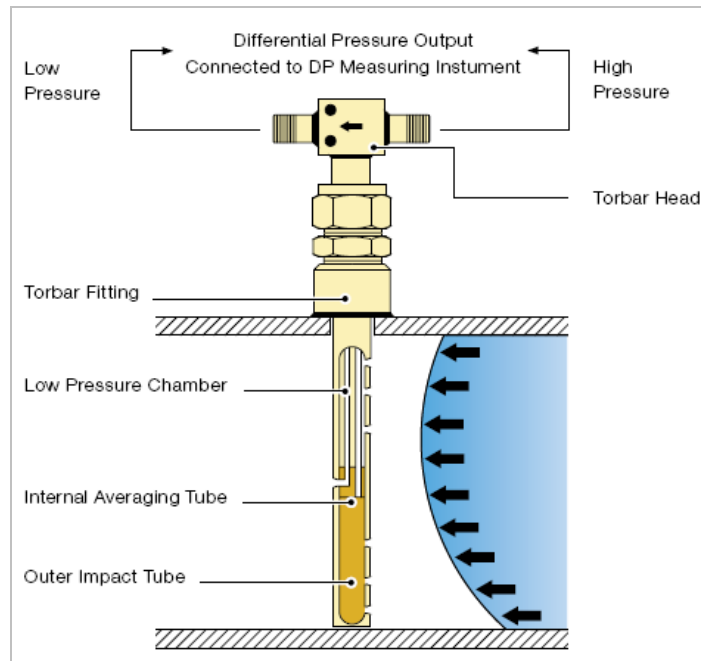


**Figure 8 Differential pressure measurement
(using the example of ABB Torbar, picture by ABB)**

The outer impact tube has a number of pressure sensing holes facing upstream which are positioned at equal annular points in accordance with a log-linear distribution. The “total pressures” developed at each upstream hole by the impact of the flowing medium are firstly averaged within the outer impact tube and then to a second order (and more accurately) averaged within the internal averaging tube. This pressure is represented at the head as the high pressure component of the differential pressure output. The low pressure component is generated from a single sensing hole located on the downstream side of the outer impact tube. For bi-directional flow measurement, the probe can be supplied with the same number of downstream ports as upstream. In general, the velocity can be computed in the same way as for Pitot tubes:

The resulting velocity is:

$$v = f_{dev.} * \sqrt{\frac{2 * p_{diff}}{\rho(p, T)}} [m / s] \quad \text{eq. (15)}$$

Where

- p_{diff} : pressure difference between averages of high (total) pressure and low pressure (s. Fig. 4.2-6.)
- v : velocity [m/s]
- $\rho(p, T)$: density of fluid
- $f_{dev.}$: device-specific factor (comprising K-factor, unit conversion factor, Reynolds number)

The device-specific factor depends also on the profile (lateral cut) of the probe. In Figure 9, an example of the flow profile around the probe is shown using the example of the ABB Torbar device.

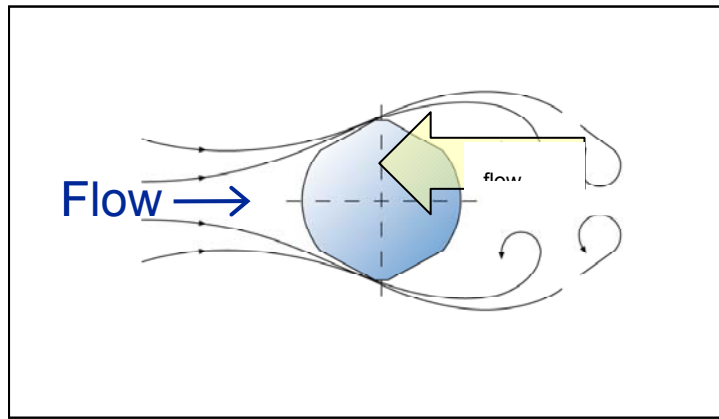


Figure 9 differential pressure measurement, flow profile around the probe (using the example of ABB Torbar; picture by ABB)

4.2.3 Thermal mass flow

Thermal mass flow meters use heat to measure flow. Thermal mass flow meters introduce heat into the flow stream and measure how much heat dissipates using one or more temperature sensors. While all thermal flow meters use heat to make their flow measurements, there are two different methods for measuring how much heat is dissipated. The method used at the wind tunnel test runs is called the constant temperature differential. Thermal flow meters using this method have two temperature sensors — a heated sensor and another sensor that measures the temperature of the gas. Mass flow rate is computed based on the amount of electrical power required to maintain a constant difference in temperature between the two temperature sensors.

Figure 410 shows the measuring principle of the thermal mass flow anemometer.

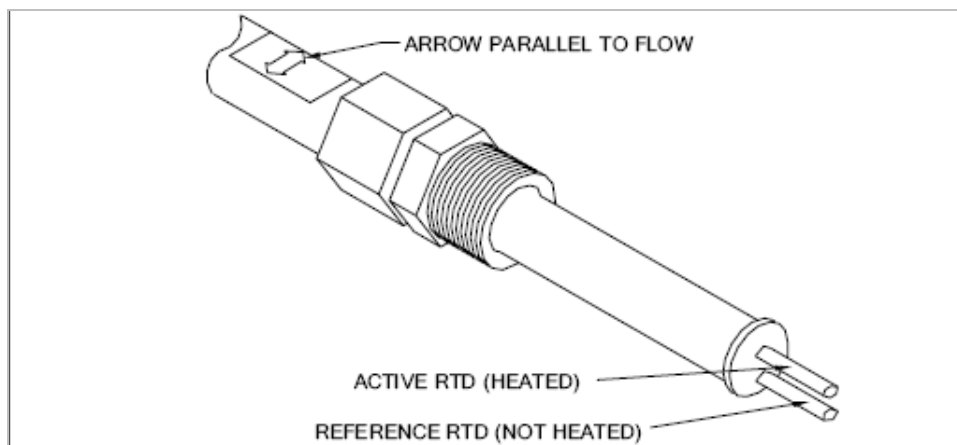


Figure 10 Flow element using the example of FCI thermal mass flow meters; RTD: resistance thermal detector (picture by FCI)

Equations 16 and 17 describe the basic computation of the flow velocity.

$$I^2 * R_S = (T_S - T_F) * (A + B * v^{0.5}) \quad (\text{King's equation}) \quad \text{eq. (16)}$$

Where

- I: electric current of sensor
- R_S: ohmic resistance
- T_S: temperature of sensor
- T_F: temperature of fluid
- A,B: constants, depending from physical ancillary conditions
- v: flow velocity normal to RTD

If the pressure is approximately constant and flow velocities less the sonic velocity the flow velocity can be computed with the following equation:

$$v = (a + b * \frac{U_{Br}^2}{T_S - T_F})^e \quad \text{eq. (17)}$$

Where

U_{Br}^2 : output Voltage of the measuring bridge
 a, b, e: constants, depending from physical ancillary conditions

Figure 11 shows the cross section of a measuring setup using the example of FCI thermal mass flow meters.

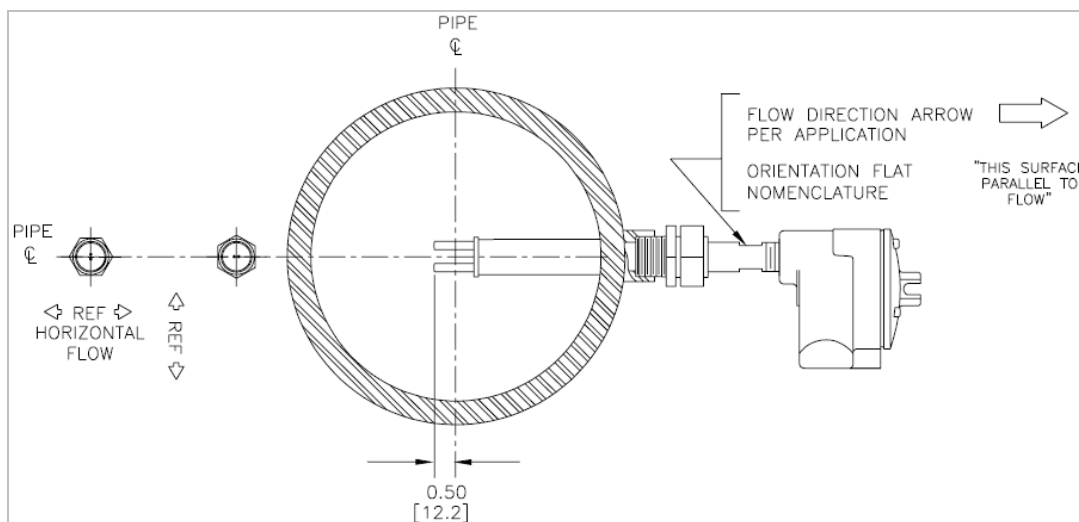


Figure 11 Measuring setup of a thermal mass flow meter (picture by FCI)

4.2.4 Vortex flow sensor

This method of flow measurement involves placing a bluff body (called a shedder bar) in the path of the fluid. As the fluid passes this bar, disturbances in the flow called vortices are created. The vortices trail behind the cylinder, alternatively from each side of the bluff body. This vortex trail is called the "Von Karman vortex street" after von Karman's 1912 mathematical description of the phenomenon.

The frequency at which these vortices alternate sides is essentially proportional to the flow rate of the fluid. Inside, atop, or downstream of the shedder bar is a sensor for measuring the frequency of the vortex shedding. With the measuring method which was used for the wind tunnel tests (Höntzsch VA 40) the vortices are measured using an ultrasonic technique.

The frequency is measured and the flow rate is calculated by the flowmeter electronics using the equation:

$$v[m/s] = \frac{f * d}{S_r} \quad \text{eq. (18)}$$

Where

f: vortex frequency
 d: characteristic length off the bluff body
 S_r : Strouhal number (constant for a given body)

The measuring method is nearly independent from density, pressure and temperature of the fluid. In normal case, a linearization of the characteristic is carried out before installation. Figure 12 shows the generally design of a vortex flow meter.

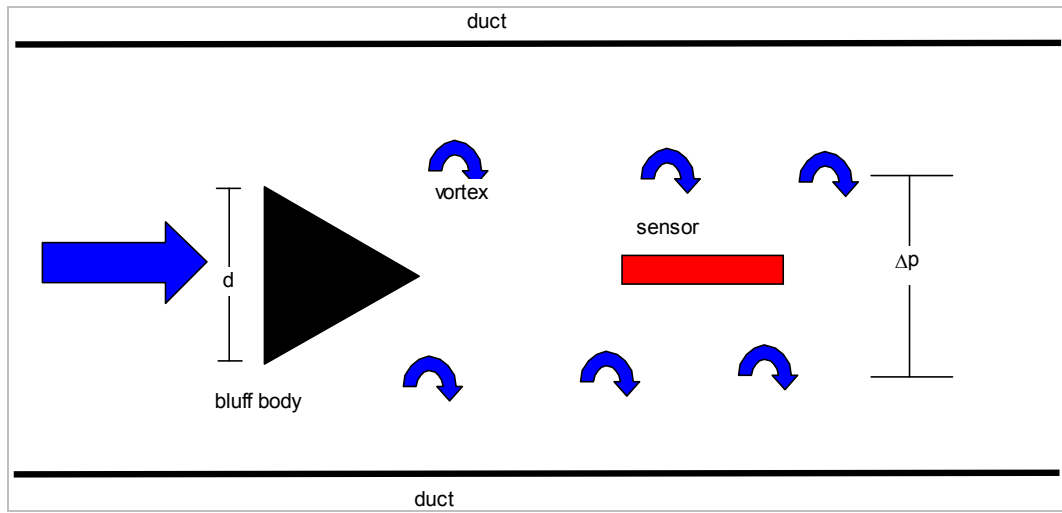


Figure 12 Vortex flow meter

In figure 13 shows an example of a vortex sensor from Höntzsch.



Figure 13 Vortex flow meter (picture by Höntzsch)

4.2.5 Vane anemometer

The measuring principle is based on the linear correlation between the rotation speed of a vane and the flow velocity. The principle is claimed to be nearly independent from ancillary conditions. In normal case, a linearization of the characteristic is carried out before installation.

$$v = f \cdot u + c \quad \text{eq. (19)}$$

Where

f, c: device-specific values
u: rotation speed

The vane anemometer is expected to be able to measure low fluid velocities down to 0,5 m/s. It is possible to measure the rotating direction so that the flow direction can be determined. Due to the very low mass of the vane, the reaction time of the anemometer can be very short.

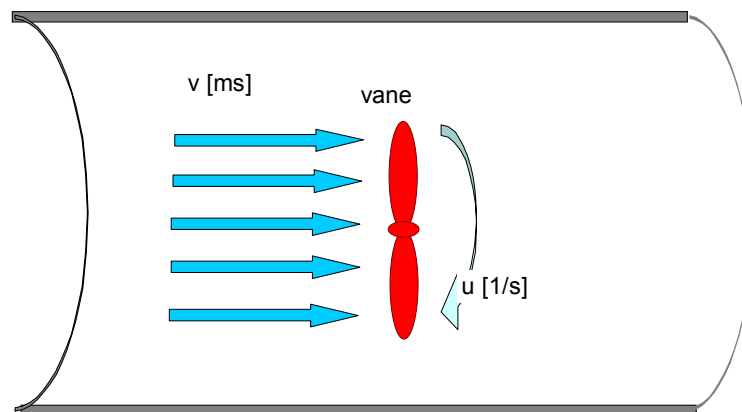


Figure 14 Vane anemometer

Figure 15 shows the vane anemometer supplied by Höntzsch FA.



Figure 15 Vane anemometer (picture by Höntzsch)

4.2.6 Time of flight (Infra-red) flow sensor - Operating Principles

The methodology employed by this AMS is closely related to the technique of measuring flow using injected of chemical dyes or radioactive tracers, where the velocity is derived from the transport time of the tracer between two measuring points a known distance apart. Instead of an artificial tracer being added to the stack gases, the naturally occurring turbulence within the gas stream is used as the tracer.

This flow turbulence causes fluctuations to occur in the infrared radiation emitted by the stack gas. This continuously variable, turbulent pattern is monitored by two passive, infra-red sensors mounted

typically one metre apart along the direction of gas flow. An electronic correlation technique is used to continuously compare the two sensor signals to determine the time delay between them imposed by the gas velocity.

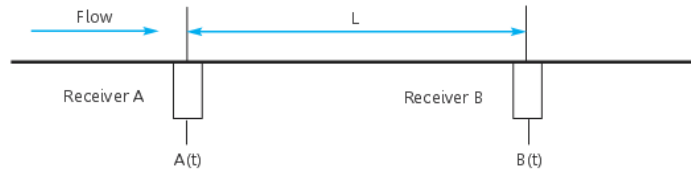


Figure 16

Typical signals from the passive infra-red sensors A and B are shown here. The signal from sensor B shows a strong similarity to that from sensor A but is delayed by a time t , the time taken for the gas to flow from point A to point B. See Figure 17

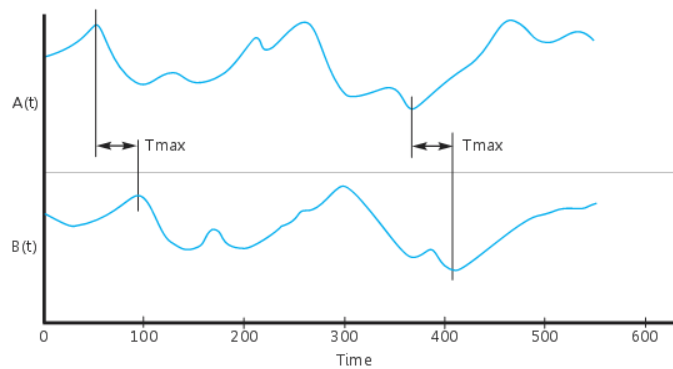


Figure 17

Continuous determination of the sensor signal time delay by the signal processor unit produces a continuous measurement of gas velocity since

$$\text{Velocity } V = L/t$$

L is the separation distance between the two sensors.



Figure 18 Installation of a Time of Flight (correlation) flow sensor

Linearity tool for the VCEM 5000 Flow Monitor

Because the signals used by the CODEL technology are derived from infra-red emissions emitted by the stack gases it is not possible to test or calibrate these devices on a standard wind tunnel using air as a medium, operating at ambient air temperatures. A flow test linearity simulator, which simulates the signals obtained on a stack, is utilised for testing, linearity checks and calibration.

5 Laboratory tests

5.1 Description of wind tunnels

5.1.1 Wind tunnel with circular cross section

The wind tunnel was sited at Technische Universität Berlin, Institut für Luft- und Raumfahrt, (TUB). The TUB provided the thermo wind tunnel, the fan for the wind tunnel and the LDA (Laser Doppler Anemometer) for the calibration of the reference L Pitot tube.

The following Figure 19 shows the construction of the wind tunnel, Figure 20 shows pictures of the actual wind tunnel. The diameter of the wind tunnel is 594mm.

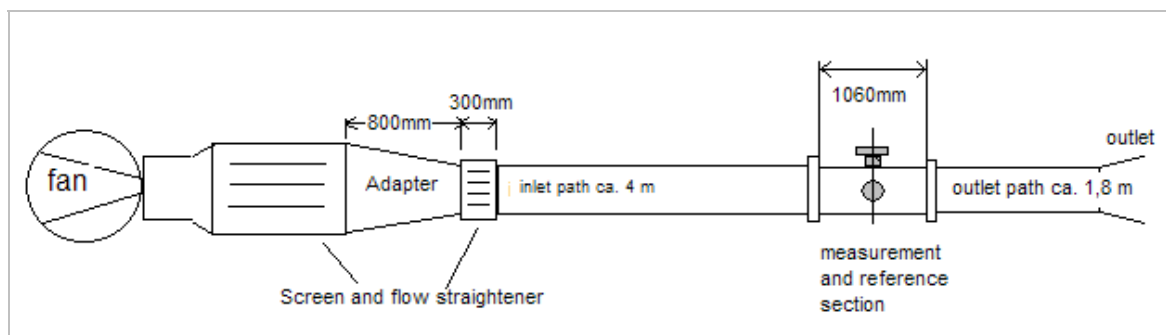


Figure 19 Wind tunnel



Figure 20 Pictures of Actual wind tunnel

Table 1 Technical specification of the wind tunnel

Item	data
fan	28 kVA dc motor
control	dc currency control unit
maximum flow (without any flow resistance)	50 m/s
maximum flow with all screens and flow straighteners	~ 25 m/s
minimum flow with all screens and flow straighteners and no flow resistance at input	~ 4 – 5 m/s
minimum flow with all screens and flow straighteners and flow resistance at input	~ 2 – 3 m/s
diameter of fan and 1. flow straightener	906 mm
diameter of wind tunnel	594 mm
length of adapter	800 mm
angel of adapter	12 °
inlet path	4.000 mm (6,7 d)
measurement section	1.060 mm
inlet in sum	~ 7,5 d
outlet path	1.800 mm (~ 3d)
outlet cone, angle	500 mm , 16,7 °
total length	~ 11.000 mm

5.1.2 Thermal (High temperature) wind tunnel

The thermal wind tunnel was sited at the TUB. Table 2 gives an overview of the technical data of the heated wind tunnel.

Table 2 Technical specification of thermal wind tunnel

Item	data
fan	19 kW ac motor
range of velocity	0 – 30 m/s
range of temperature	293 – 773 K
intensity of turbulence	0.3 – 0.4 %
Reynolds number (l = 1 m)	$2 * 10^6$
measuring section	320 x 225 x 1700 mm
type	“Göttinger Umlaufkanal”

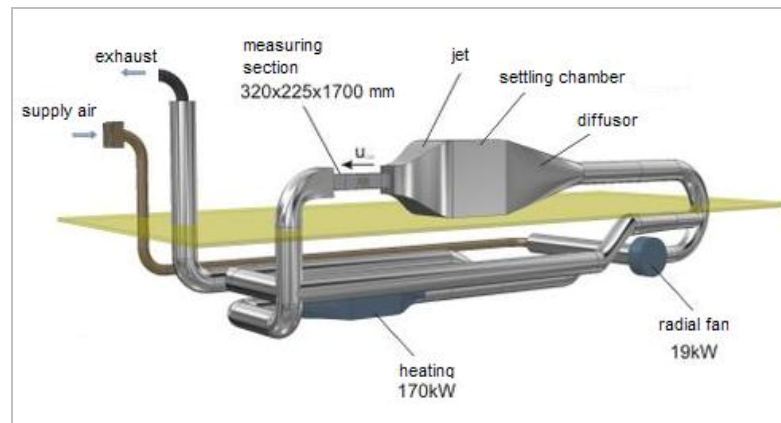


Figure 21 Setup of the thermo wind tunnel

5.2 Description of the lab tests

The following test program had been carried out. Table 3 presents an overview of the carried out tests.

Table 3 Laboratory tests

wind tunnel	method	device	description	number/type of measurements	date
circular	manual	L Pitot	calibration of L Pitot against LDA	53 test runs as single point measurements	10.02.2010 and 19.05.2010
circular	manual	L Pitot	reproducibility measurements of two L Pitot against the calibrated L Pitot	100 test runs as single point measurements at 5, 10, 15, 20 and 25 m/s; at a time 10 test runs per velocity and 40 test runs as single point measurements at 4 and 3 m/s	25.02.2010
circular	manual	L Pitot	measuring of the flow profile against reference (single point)	10 test runs at 2 axis (coextensive) at a time 2 test runs at 5, 10, 15, 20, 25 m/S	25.02.2010
circular	manual	L Pitot	testing of yaw and pitch	14 test runs at several angels at about 10 m/s	25.02.2010
circular	manual	S Pitot	reproducibility measurements of two S Pitot against the calibrated L Pitot	100 test runs as single point measurements at 5, 10, 15, 20 and 25 m/s; at a time 10 test runs per velocity and 40 test runs as single point measurements at 4 and 3 m/s	26.02.2010
circular	manual	S Pitot	measuring of the flow profile against reference (single point)	10 test runs at 2 axis (coextensive) at a time 2 test runs at 5, 10, 15, 20, 25 m/S	26.02.2010
circular	manual	S Pitot	testing of yaw and pitch	14 test runs at several angels at about 10 m/s	26.02.2010

wind tunnel	method	device	description	number/type of measurements	date
circular	manual	3D-Pitot	reproducibility measurements of two 3d- Pitot and 2 calibration methods against the calibrated L Pitot	200 test runs as single point measurements at 5, 10, 15, 20 and 25 m/s; at a time 10 test runs per velocity and 40 test runs as single point measurements at 4 and 3 m/s	22.02.2010 - 24.02.2010
				12 test runs at 2 axis (coextensive) at a time 2 test runs at 5, 15, 25 m/S with 2 calibration methods	23.02.2010
circular	automatic	Torbar / ABB	reproducibility measurements of two test runs against the calibrated L Pitot	100 test runs as single point measurements at 5, 10, 15, 20 and 25 m/s; at a time 10 test runs per velocity and 60 test runs as single point measurements at 4, 3 and 2 m/s	04.03.2010
circular	automatic	ultrasonic cross duct/SICK	reproducibility measurements of two test runs and two devices against the calibrated L Pitot	100 test runs as single point measurements at 5, 10, 15, 20 and 25 m/s; at a time 10 test runs per velocity and 30 test runs as single point measurements at 4, 3 and 2,5 m/s	01.03.2010
circular	automatic	ultrasonic single probe/SICK	reproducibility measurements of two test runs against the calibrated L Pitot	100 test runs as single point measurements at 5, 10, 15, 20 and 25 m/s; at a time 10 test runs per velocity and 30 test runs as single point measurements at 4, 3 and 2,5 m/s	05.03.2010
circular	automatic	Vortex shedding/Höntzsch	reproducibility measurements of two test runs and two devices against the calibrated L Pitot	100 test runs as single point measurements at 5, 10, 15, 20 and 25 m/s; at a time 10 test runs per velocity and 50 test runs as single point measurements at 4, 3 and 2 m/s	02.03.2010
circular	automatic	vane anemometer/Höntzsch	reproducibility measurements of two test runs and two devices against the calibrated L Pitot	100 test runs as single point measurements at 5, 10, 15, 20 and 25 m/s; at a time 10 test runs per velocity and 60 test runs as single point measurements at 4, 3 and 2 m/s	08.03.2010
circular	automatic	thermal mass flow/ FCI	reproducibility measurements of two test runs and two devices against the calibrated L Pitot	100 test runs as single point measurements at 5, 10, 15, 20 and 25 m/s; at a time 10 test runs per velocity and 60 test runs as single point measurements at 4, 3 and 2 m/s	08.03.2010

wind tunnel	method	device	description	number/type of measurements	date
				56 test runs at 25 °C (6), at a time 10 measurements at 60 °C, 202 °C, 333 °C, 160 °C and 238 °C at 24.02.2010	
heated	manual	S Pitot/ L Pitot	temperature dependency	90 test runs at 20 °C, 40 °C, 129 °C, 167 °C, 196 °C, 225 °C; 262 °C AND 290 °C at 22.12.2010	24.02.2010

Due to the dimensions of the wind tunnel and the local circumstances it was not possible to determine the repeatability in parallel measurements (possible interferences between the devices). It was also necessary to do parallel measurements with the reference L Pitot.

In order to make the measurements comparable, the statistical evaluation for the repeatability was carried out with the regression lines between the AMS and the reference method standardized on the target value (see Chapter 8)

The profile measurements with the manual methods occurred against the reference method. The measured profiles had been normalized on the reference.

Refer to document CEN TC 264 WG23 N 225 Final report of Muller lab tests M81522_04_BER_4D for full details of the test and results.

A further series of tests were conducted on the thermal wind tunnel, to attempt to confirm earlier observations on the behavior of the Pitot tubes at temperatures above 200 °C. These tests are reported in N235a ref to Muller report.

These tests did not reproduce the non-linear behavior of the Pitot flow measurements above 200 °C. The summary of the tests was that the velocities which were measured with the vane anemometer, the L Pitot and the S Pitot were nearly constant over the tested temperature range (20 – 290 °C). The deviation against the reference added up to 1 m/s (L Pitot) resp. 0,5 m/s (S Pitot) at 11 m/s and 0,5 m/s (S+L Pitot) at 21 m/s. The standard deviation of the velocity of the different devices at all test runs were on a low level under 0,1 m/s.

6 Field tests

6.1 Copenhagen (waste incinerator)

The first validation field trial for stack gas velocity/flow measurement was conducted at a waste incinerator in Copenhagen in May 2010. The incinerator was operating with three combustion lines feeding a shared stack of 2.8 m internal diameter. The stack gas is typically at 130°C at 10% O₂ dry and contains about 20% water vapour. The bulk velocity was circa 20 m/s during the tests.

Two measurement platforms were available at about four and twenty stack diameters from the stack inlet. Four test teams performed 20 point velocity traverses using L type, S type, and Spherical (3D) Pitots and a vane anemometer. Two tracer methods were also employed – a transit time method using a radioactive tracer and a dilution method using nitrous oxide and methane tracer gases.

The Pitot measurements at the lower level indicated very non-uniform velocity profiles when compared with the very uniform profiles obtained at the upper level which approached the fully developed condition. Despite this, representative bulk velocity averages were obtained in both cases. This indicates that the location of manual testing does not need to be at a very uniform flow location.

The L and S type Pitots and the vane anemometer gave comparable results for bulk velocity. The 3D Pitot was about 3% lower and agreed with the radio-active tracer and dilution tracer results (using nitrous oxide injection). The level of swirl in the flow was very low.

Various CEMs were installed for the trial and these demonstrated linear performance in a tolerance band of about $\pm 10\%$ at 20 m/s when compared with the tracer result. The manual measurements interfered with downstream CEMs that were vertically aligned with the sample ports.

6.1.1 The field trial

The stack velocity and flow rate measurement campaign was conducted at the Amagerforbraending waste incinerator site in Copenhagen. There are four separate incineration lines firing mixed waste (mostly municipal), each fitted with NO_x abatement (SNCR), particulate abatement (bag filters) and individual continuous emission monitoring (CEM) systems. Only three lines were operational during the trials.

The exhaust ducts from the individual lines feed a joint stack of 2.8m internal diameter. Velocity traverses were conducted at two stack heights of about 20m and 60m above ground level. Tracer methods were also used to determine the velocity (a time-of-flight method with radio-active tracer) and stack gas flow rate (dilution method using CH₄ and N₂O tracer gases).

Refer to document CEN TC 264 WG23 N 226 Final Copenhagen field trial report for full details of the tests and results.

6.2 Wilhelmshaven (coal fired power plant)

The second validation field trial for stack gas velocity/flow measurement was conducted at a 700 MW electric coal fired power plant in Wilhelmshaven in July 2010. The single power plant boiler has two FGD units that feed a shared stack of 7m internal diameter. The stack gas is typically at 120°C at 6% O₂ dry and contains about 12% water vapour. The bulk velocity ranged from 24 to 31 m/s during the testing and the level of swirl in the flow was again very low.

One measurement platform was available at about 6.5 stack diameters from the stack inlet. Four test teams performed 20 point velocity traverses using paired trains of L type, S type, Spherical (3D) and 2G Pitots. The L type Pitots were strapped together and inserted through a single port. It was not possible to use tracer methods at this plant due to the difficulty in obtaining permission to use a radio-active tracer and the poor mixing quality obtained for dilution flow methods.

The Pitot measurements indicate non-uniform velocity profiles. Despite this, representative bulk velocity averages were obtained, confirming the previous field trial results.

The L, S type and 3D Pitots gave comparable results for average velocity with the 3D Pitot being about 1% lower than the L type and showing a greater difference between the two trains. The L type showed the least variation between trains as might be expected since they were nominally measuring at the same point. These results agree with the plant flow rate calculated from the electricity generation and the plant efficiency. The installed flow CEM, a Sick ultra-sonic cross-duct flow meter, also agreed closely with the measurements. A Codel correlation based flow meter, installed at a lower level in the stack, compared well but read about 6% lower (without calibration).

6.2.1 The field tests

The stack velocity and flow rate measurement campaign was conducted at the E.ON Kraftwerke 700 MWe coal fired power plant in Wilhelmshaven, Germany. The flow from the boiler is split between two abatement trains, each with Electrostatic precipitators, NO_x removal (SCR) and wet Flue Gas Desulphurisation (FGD).

The exhaust ducts from the abatement lines feed a joint stack of 7m internal diameter. Velocity traverses were conducted at the 52.3m level in the stack.

The test schedule was badly affected by an unexpected plant shut-down due to a boiler tube leak on the morning of DAY 3 (7th July) during the fourth velocity traverse. Testing was therefore abandoned and testing resumed during week commencing Monday 19th July. A total of 11 full traverses was obtained for the L type, S type and 3D Pitots and 10 traverses for the 2G type, all using paired trains.

The actual programme of velocity traverses was different to the plan as shown in Appendix C. In the first test week, 3 traverses were conducted simultaneously using the L, S and 3D Pitots operated by NPL, Muller and E.ON respectively. These are designated T1, T2 and T5 in line with the original plan. The plant shut-down occurred during the next traverse (designated T6) for which the partial results were recorded but not counted for flow rate determination. The 2G Pitots were also operated by Astech for T2/T5/T6 and Hoentzsch used a single vane anemometer probe for T5/T6 only.

Re-scheduling of the testing was problematic so the remainder of the traverses (T7 to T14) were not conducted simultaneously since the various test teams could not attend site at the same times in week commencing 19th July. The L type and 3D testing was undertaken simultaneously on the 20th and 21st July but the L type Pitots were operated by E.ON since NPL was not available. Astech also conducted 2G Pitot measurements on 20th and 21st July with some simultaneous measurements and some independent measurements (due to late arrival). Muller conducted the same traverses separately on 22nd and 23rd July. Hoentzsch was not able to attend site.

E.ON had visited the site week commencing 28th June to supervise the installation of trial CEMs for velocity measurement, to organise the data logging (all parameters logged at 1s intervals) and to conduct some preliminary duct surveys ahead of schedule. The two-man lift again caused time delays.

Refer to document CEN TC 264 WG23 N 227 Final Wilhelmshaven field trial report for full details of the tests and results.

7 Analysis of validation studies

7.1 Introduction

This section of the validation report summarises the statistical performance of the methods determined from the laboratory and field test programme, the full statistical analysis is discussed in the Validation Study Analysis Report [CEN TC 264 WG23 N238].

The performance characteristics which have been determined include:

- Lack of fit (Laboratory)
- Repeatability Uncertainty (Laboratory)
- Reproducibility (Field)
- Repeatability Uncertainty (Field)

In addition the methodology for calibration the continuous flow measuring instruments (AMS) using a manual method was validated. This involved determining the calibration function for the AMSs using the QAL2 procedure defined in EN 14181 Stationary Source Emissions - Quality assurance of automated measuring systems.

7.2 Overview of techniques assessed in validation studies

Table 4 provides a summary of the different manual methods, and Table 5 provides a summary of the different AMS instruments, which were deployed in the three phases of the validation studies, the laboratory tests and the two field campaigns. Where several implementations of a method have been used, these are labelled for example as L1 and L2 for two L Type Pitots.

Manual	Laboratory Tests	Field Test 1	Field Test 2
--------	------------------	--------------	--------------

(discontinuous) methods	'Copenhagen'		'Wilhelmshaven'
	Methods used	Methods used	Methods used
Differential pressure devices			
L Type Pitot	L1, L2	L1, L2, L3,L4 ^(a)	L1, L2
S Type Pitot	S1, S2	S1, S2	S1, S2
3D Pitot	3D1, 3D2	3D1, 3D2	3D1, 3D2
2G Pitot			2G2,2G1
Vane anemometer	V1, V2	V1, V2	V1
Tracer Gas measurement			
Transit Time (radioactive)		Tracer- Transit Time	
Dilution		Tracer - Dilution	
Calculation from plant/process data			Plant

Table 4 Summary of techniques assessed in validation studies

- a. *Due to the way the L type pitots were deployed in the first field trial, the data from L1/L2 was combined to give complete traverses of the duct, and so parallel data were not available from paired instruments.*
- b. *Because of issues caused by the Icelandic volcano affecting travel in Europe, the Averaging Pitot was not deployed in time for the field tests. The AMSs were left operating after the period of the study, and parallel data was obtained with the averaging Pitot and other AMSs, which has allowed an assessment of the averaging pitot performance.*

Automated Measuring Systems AMS (instruments)	Laboratory Tests	Field Test 1	Field Test 2
	Instruments used	'Copenhagen' Instruments used	'Wilhelmshaven' Instruments used
Ultrasonic, Cross Duct	UCD1(single path), UCD2(double path)	UCD1 (60m single path), UCD2 (20m double path)	UCD
Ultrasonic, Probe	USP	USP (60m)	
Differential pressure measurement, Cross Duct (Averaging Pitot)	AP	AP ^(a)	
Thermal mass flow	TMF1, TMF2		TMF

(probe)			
Vortex shedding (probe)	VOR1, VOR2	VOR5, VOR8	VOR
Vane anemometer (probe)	VAN1, VAN2	VAN	VAN
Correlation Time of Flight AMS			COR

Table 5 Summary of techniques assessed in the validation studies

- a) Because of issues caused by the Icelandic volcano affecting travel in Europe, the Averaging Pitot was not deployed in time for the field tests. The AMSs were left operating after the period of the study, and parallel data was obtained with the averaging Pitot and other AMSs, which has allowed an assessment of the averaging pitot performance.

As can be seen from Table 1 and Table 2, not all methods were available for all the validation phases. This was due to instrument availability, plant infrastructure, and other logistical issues.

In addition during the first field validation study the L Type Pitots did not produce parallel measurements of average duct flow. In the second field trial, the L Type Pitots were linked together to provide paired measurements of the same area of the duct, and so repeatability data can be obtained from these measurement sets.

7.3 Summary of performance data from laboratory studies

This section summarises the statistical performance of the methods assessed during the laboratory test programme. Details of the tests and the statistical analysis are given in the laboratory test report Ref CEN TC 2264 WG23 N235, produced by Muller BBM. The results of these statistical tests are repeated here for completeness. Additional analysis has been carried out by NPL to assess the lack of fit performance of the methods, in accordance with EN 15267-3. Validation tests were carried out on a wind tunnel over the range 5 -25 m/s.

7.3.1 AMS performance in laboratory validation study

Linear regression analysis was carried out on the AMS results, and the results are summarised in Table 6. Two calibration functions are given for each type of AMS, one for each pair. It can be seen that, not surprisingly, the paired instruments have similar calibration functions to each other.

AMS	Principle	Calibration function	
		Slope	Intercept
AP	Differential pressure – cross duct	1.058	-0.220
		1.067	-0.434
UCD	Ultrasonic – cross duct	1.048	-0.021
		1.050	-0.365
USP	Ultrasonic - probe	1.124	-0.016
		1.120	-0.056
TMF	Thermal mass measurement - probe	1.019	-0.061

		1.100	-0.348
VAN	Vane anemometer – probe	0.970	0.227
		0.990	0.226
VOR	Vortex shedding – probe	1.010	-0.409
		0.980	0.379

Table 6 AMS calibration functions from the Laboratory tests

Table reproduced from CEN TC 2264 WG23 N235, Muller BBM.

The uncertainties due to bias u_B and the uncertainties $u(y)$ of the AMSs laboratory study data were determined in accordance with EN ISO 20988 and are summarised in Table 7. In addition the expanded uncertainty expressed with a 95% level of confidence $U_{0.95}$ is also given. The AMSs all pass the criteria given in ISO EN 20988 for u_B which is used as a measure of the validity of the uncertainty assessment.

	Bias	Bias Criteria	Uncertainty	Expanded uncertainty	Coverage factor	Valid Test
Technique	u_B		u	$U_{0.95}$	k	
AP	0.0002	0.236	0.035	0.042	2	Y
UCD	0.003	0.237	0.090	0.180	2	Y
USP	0.0002	0.236	0.033	0.066	2	Y
TMF	0.01	0.239	0.138	0.275	2	Y
VOR	0.001	0.236	0.051	0.101	2	Y
VAN	0.004	0.236	0.021	0.042	2	Y

Table 7 Summary of uncertainties determined for AMS from the laboratory studies

7.3.2 Manual method performance in laboratory validation study

The performance of the manual methods assessed during the laboratory test programme is summarised in Table 8 which presents the linear regression of the methods, and Table 9 which summarises the uncertainty assessment of the methods from the laboratory study. Two results are provided for the 3d-Pitots (ES and AP), which relate to two different calibration factors provided using two different suppliers/approaches. This is explained in more detail in the laboratory test report.

Table 10 presents the lack of fit data which has been determined from the laboratory regression studies, in accordance with the procedure given in EN 15267-3. This quantifies lack of fit as the largest (absolute) deviation from the determined regression line of any single measurement data point. For illustrative purposes the lack of fit has also been compared against the criterion for lack of fit given in EN 15267-3, which is 3% of the testing range.

Method	Technique	Slope	Intercept
3d Pitot (ES)	Differential pressure 3- axis	0.996	-0.222 m/s
		1.002	-0.652 m/s
3d Pitot (AP)	Differential pressure 3-axis	1.012	-0.229 m/s
		1.051	-0.716 m/s
S type Pitot	Differential pressure	0.830	-0.286 m/s
		0.833	-0.205 m/s
L type Pitot	Differential pressure	1.025	-0.500 m/s
		1.008	-0.160 m/s

Table 8 Linear regression data for manual methods from laboratory test data

	Bias	Bias	Uncertainty	Expanded	Coverage	Valid
--	------	------	-------------	----------	----------	-------

		Criteria		uncertainty	factor	Test
Technique	u_B		u	$U_{0.95}$	K	
3d Pitot (ES)	0.0002	0.246	0.252	0.504	2	Y
3d Pitot (AP)	0.006	0.247	0.261	0.522	2	Y
S Type Pitot	0.005	0.238	0.108	0.216	2	Y
L Type Pitot	0.100	0.278	0.503	1.006	2	Y

Note: A possible explanation for the relatively higher bias and uncertainty observed for the L type Pitot has been proposed by MBBM that it may have been due to use of different electronic pressure reading devices during the test programme. The importance of the use of traceable, calibrated pressure reading devices, with appropriate ranges, has been taken on board in the drafting of the standard.

Table 9 Uncertainty analysis for manual methods in laboratory assessment

Technique	Lack of fit As percentage of testing range (25 m/s)	Criteria (From EN15267-3)
L1	0.78 %	3 %
L2	0.97 %	3 %
3d1 (ES)	1.14 %	3 %
3d2 (ES)	0.91 %	3 %
3d1 (AP)	1.12 %	3 %
3d2 (AP)	0.87 %	3 %
S1	1.73 %	3 %
S2	2.57 %	3 %

Table 10 Lack of fit determined from laboratory test data for manual methods

7.4 Performance evaluation of field test 1 'Copenhagen'

A full description of the field tests, including description of the test site, and the experimental design, and data analysis, is given in the field test report "CEN Working Group 23: Stack Gas Velocity Standards, First validation field trial: Copenhagen (waste incinerator)" produced by E.ON New Build & Technology (subsequently referred to herein as the 'first field validation study report').

As described in the first field validation study report, validation measurements were carried out at two sampling planes at different stack heights, and so not all methods were co-located. However, there should be no change in the stack volumetric flow between these locations, so parallel assessment of the tests can be performed. It should be noted that the lower height sampling plane (20m) had perturbed flow profile, as it was only 4.3 stack diameters down stream of the 90 degree turn in the flow at the stack inlet point (as described in the first field validation study report).

During the test period the AMS results were logged for the whole period. Owing to issues with travel disruption due to the eruption of the Eyjafjallajökull volcano, the ABB Torbar averaging Pitot could not be installed until after the period of the parallel manual-method tests. However, the AMSs were kept installed and a period of parallel measurements between all the AMSs was recorded. These data enable a comparison to be made between all the installed AMSs.

The main data sets available for performance assessment are those during which the manual methods were used to obtain average flow measurements. These measurements involved determining the flow velocity across the duct and averaging these data to obtain a volumetric flow for the duct, representative of the sampling period. For the S type and 3d Pitot methods, ten flow measurements were made. During these periods the AMS data have been averaged to provide comparable data sets. Due to the way the measurements using the L type Pitots and manual vane anemometer were carried out, these produced 21 average flow measurements. However, for the L type measurements, the flow measurements across the duct were determined using two L type pitots to build the average flow, and so parallel average flow data are not available for pairs of L type Pitots. Also, because of the scheduling of the tests, only seven of the L type and five of the

vane average flow measurements match periods for which the S type and 3d Pitot produced average flow measurements.

In addition, to obtain further comparison data, the AMS data have been averaged over the 21 periods of L type and vane measurements. Tracer measurements were carried out over a smaller number of periods coincident with test runs, and these gave 4 periods of parallel dilution tracer measurements and four periods of radioactive tracer measurements that match 3d and S type measurement periods.

Tables 11 and 12 summarise the parallel data sets that have been assessed for the the 21 L type Pitot and vane measurement periods and the 10 S type and 3d Pitot measurement periods . Note that data points corresponding to L type Pitot test periods 12 and 18, as defined in the first field validation test report, have been removed due to outliers. It is interesting to note that test 18 was performed at the 60m test height, and this may have led to a systematic difference. This is being investigated further to check if there is any influence factor that needs to be taken into account in the drafting of the standard.

The AMS systems were not calibrated when installed, and so it is expected that there are systematic differences between the raw AMS data. Figure 22 presents a plot of the data sets in Table 11, and Figure 23 presents a plot of the data sets in Table12.

As can be seen from these plots, there are significant systematic differences between the AMS systems, which is to be expected, as these systems were not calibrated. The manual methods (indicated on the graph by dotted lines) in general show much closer agreement.

Test Identifier	Corresponding test in field test report	Date	Start time	End time	UCD1 m/s	UCD2 m/s	UPR m/s	VOR5 m/s	VOR8 m/s	VAN m/s	L Type m/s	Manual vane m/s	Radioactive Tracer m/s
L1	1a	18/05/2010	10:24	13:23	20.00	-	17.76	18.92	21.05	21.08	19.63	-	-
L2	1b	18/05/2010	10:38	13:44	20.29	-	18.00	19.10	21.27	21.32	19.71	-	-
L3	2a	18/05/2010	15:02	18:31	20.89	17.24	18.53	19.75	21.95	22.00	20.10	-	19.17
L4	2b	18/05/2010	15:29	18:34	21.02	17.36	18.64	19.90	22.12	22.13	20.06	-	19.31
L5	3	19/05/2010	08:53	09:23	20.28	16.69	17.94	19.06	21.15	21.19	19.61	-	-
L6	4	19/05/2010	10:32	11:07	20.49	16.83	18.10	18.51	21.48	20.64	19.91	19.99	19.30
L7	5	19/05/2010	11:15	11:56	20.65	16.92	18.26	18.02	21.57	20.13	19.99	20.09	-
L8	6	19/05/2010	12:04	12:36	20.69	16.93	18.38	16.57	21.73	17.62	19.85	19.92	-
L9	7	19/05/2010	13:35	14:01	20.40	16.80	18.05	18.06	21.46	20.16	19.77	20.03	-
L10	8	19/05/2010	14:16	14:52	20.40	16.78	18.06	17.30	21.42	19.63	19.68	20.03	-
L11	9	19/05/2010	15:02	15:41	19.94	16.31	17.70	15.95	20.98	17.51	18.88	19.29	-
L12	10	19/05/2010	15:47	16:22	19.88	16.27	17.60	13.06	20.91	19.33	19.20	19.46	18.69
L13	11	19/05/2010	16:28	17:02	18.53	15.19	16.30	11.31	19.35	18.10	17.50	17.74	14.92
L14	13	20/05/2010	09:00	09:27	20.19	16.66	17.89	17.42	21.17	19.44	19.18	19.66	-
L15	14	20/05/2010	09:33	10:02	20.18	16.60	17.92	16.90	21.22	18.90	19.58	19.82	-
L16	15	20/05/2010	10:05	10:31	20.26	16.73	17.91	18.35	21.24	20.61	19.63	19.71	-
L17	16	20/05/2010	10:36	11:01	20.29	16.59	17.94	16.57	21.20	17.89	19.46	19.47	-
L18	17	20/05/2010	11:02	11:26	19.70	16.24	17.43	16.93	20.73	18.32	19.10	19.02	-
L19	19	20/05/2010	13:57	14:23	21.07	17.30	18.57	17.82	22.08	19.92	20.35	20.41	-
L20	20	20/05/2010	14:26	14:49	20.45	16.79	18.07	16.99	21.42	19.18	19.77	19.83	-
L21	21	20/05/2010	14:57	15:02	19.84	16.24	17.43	17.91	20.75	20.04	19.15	19.09	-

Table 11 Comparable data sets for time periods of L Type and vane manual methods

Test Identifier	Corresponding test in field test report	Date	Start time	End time	UCD1 m/s	UCD2 m/s	UPR m/s	VOR5 m/s	VOR8 m/s	VAN m/s
S1	2a	18/05/2010	15:23	18:31	20.89	17.27	18.53	19.74	21.98	21.99
S2	2b	18/05/2010	15:29	18:34	21.00	17.35	18.62	19.86	22.07	22.07
S3	3	19/05/2010	10:25	11:59	20.62	16.96	18.29	17.95	21.58	20.14
S4	4	19/05/2010	13:22	14:59	20.50	16.83	18.15	17.93	21.52	19.94
S5	5	19/05/2010	15:31	17:07	19.21	15.75	17.02	14.53	20.18	18.91
S6	6	19/05/2010	17:22	18:03	19.98	16.35	17.64	17.47	20.93	19.49
S7	7	20/05/2010	9:09	10:36	20.17	16.63	17.84	17.59	21.13	19.73
S8	8	20/05/2010	11:12	12:40	20.08	16.56	17.77	17.55	21.09	19.57
S9	9	20/05/2010	14:11	15:22	20.43	16.76	18.02	17.86	21.40	19.81
S10	10	20/05/2010	15:25	16:45	20.06	16.53	17.71	17.39	21.02	19.57

3D1 m/s	3D2 m/s	S Type 1 m/s	S Type 2 m/s	Manual vane m/s	L Type m/s	Dilution tracer m/s	Dilution tracer m/s	Radioactive tracer m/s
20.05	20.02	21.10	19.84	-	20.10	-	-	19.24
20.23	20.07	21.18	20.05	-	20.06	-	-	19.24
19.08	19.23	19.83	20.38	20.04	19.95	-	18.97	19.36
18.91	19.22	19.73	20.32	20.03	19.72	19.40	-	-
17.84	17.78	18.36	19.03	18.60	18.35	-	17.34	17.61
17.89	19.20	19.21	19.44	-	-	-	-	-
18.52	19.15	19.29	19.38	19.73	19.46	19.00	-	-
18.44	18.85	19.35	19.31	-	-	19.00	-	-
18.80	19.30	19.81	19.76	19.46	19.46	-	-	-
18.43	18.82	19.28	19.28	-	-	-	-	-

Table 11 Comparable data sets for time periods of S and 3d manual methods

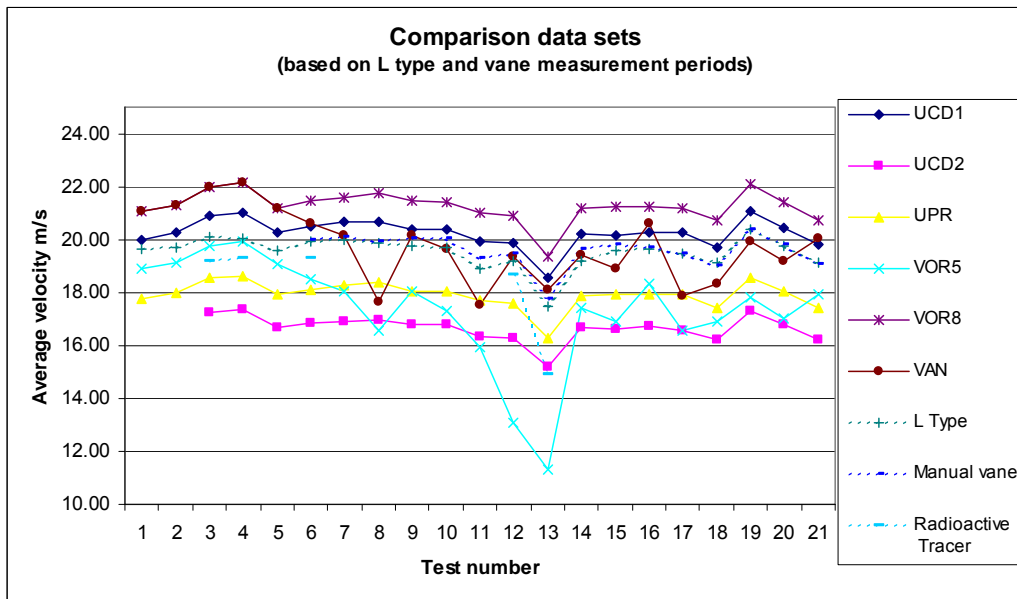


Figure 22 Plot of raw data for L type and vane measurement periods

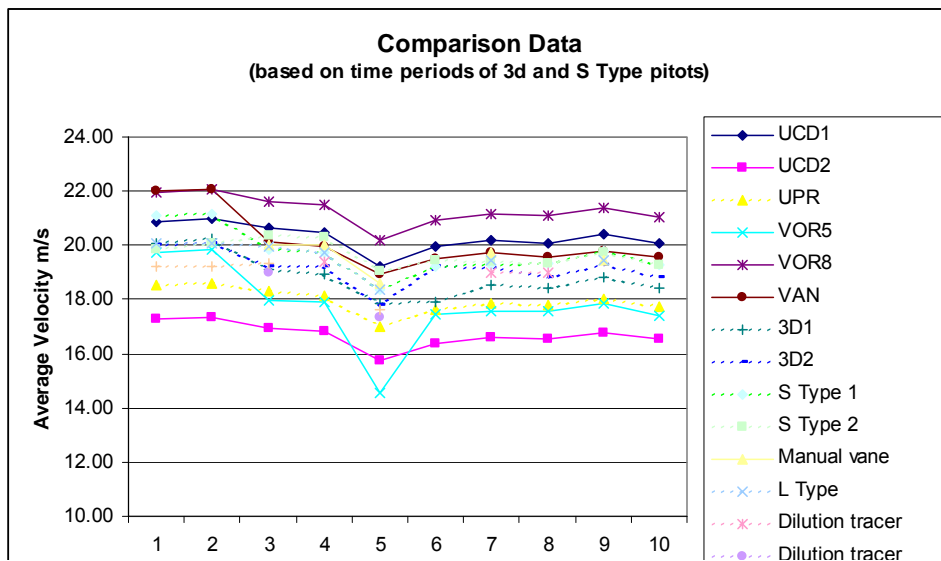


Figure 23 Plot of raw data for S Type and 3D Pitot measurement periods

7.4.1 Repeatability and uncertainty of manual methods in the first field validation study.

In order to provide an assessment of the repeatability of the manual methods in the first field validations study, the paired sets of data for the 3d and S Type Pitots were assessed in accordance with the procedure in CEN TS 14793:2005 which provides a method to determine the pooled standard deviation of paired results. (Paired data was not available for the L type Pitot and vane anemometers) This was done by determining the standard deviation of each pair of measurements and then combining those as variances (i.e. mean sum of squares). This assessment includes the effects of any systematic differences between the methods.

In order to assess the ensemble standard deviation of all of the manual methods, the standard deviation of each set of coincident 3d, S type, vane and L type results was determined and the pooled standard deviation for all these sets of measurements was calculated, again in accordance with the approach given in CEN TS 14793. In addition the pooled standard deviation for the paired 3d and paired S type pitots were determined. The results of these tests are given in Table 13

Pooled standard deviations of manual methods			
All methods including tracers		All manual Pitot methods	
Mean	19.31 m/s	Mean	19.35 m/s
Pooled stdv	0.51 m/s	Pooled stdv	0.50 m/s
k	2.00	k	2.00
U(95)	1.03 m/s	U(95)	1.00 m/s
Rel stdv	2.66 %	rel stdv	2.57 %
Urel(95)	5.33 %	Urel(95)	5.15 %
Paired S Type Pitot		Paired 3d Pitots	
Mean	19.70 m/s	Mean	18.99 m/s
Pooled stdv	0.45 m/s	Pooled stdv	0.38 m/s
k	2	k	2.00
U(95)	0.90 m/s	U(95)	0.75 m/s
Rel stdv	2.28 %	Rel stdv	1.98 %
Urel(95)	4.57 %	Urel(95)	3.97 %

Table 12 Pooled standard deviations of manual methods in the field

These results have been determined from the coincident tests (10 periods), although only a limited number of data points are available for some of the methods. The standard deviations include both random and systematic variations, although as the methods are intended to provide traceable results for calibration of AMS, inter-method biases should be expected to be small. The measurements have also been made at different sample locations (60m and 20m elevations) and so this analysis also includes any variability caused by the different sampling configurations. Care should therefore be taken in interpreting these results.

The pooled standard deviation for measurements made using the L type Pitot and the manual vane anemometer was also calculated (Table 14). This analysis used all 18 paired measurement periods made using these two methods.

Pooled standard deviation Paired L type and vane	
Mean	19.50 m/s
Pooled stdv	0.22 m/s
k	2.00
U(95)	0.43 m/s
Rel stdv	1.10 %
Urel(95)	2.21 %

Table 13 Pooled standard deviation for L Type and vane anemometers

The uncertainty of the manual methods was assessed using the techniques defined in ISO EN 20988. As it is proposed that any of the manual approaches can be used to calibrate the AMS techniques, in this analysis we consider the set of manual methods as implementations of a single method. In this way the uncertainty of the ensemble of the methods is determined. The results can therefore be interpreted as the uncertainty for any of the manual methods, though of course if any of the methods have a better performance this will be masked by the ensemble performance. The set of parallel measurements can be considered as an experimental design conforming to experimental design A8: parallel measurements with identical measuring systems, defined in ISO EN 20988. Where 'identical' in this context is taken to mean complying with the requirements of the manual method standardised by WG23. This assumes the uncertainties of the different implementations of the method are similar (the assumption is that all the results from the techniques represent samples of an overall population of results representing 'the method' as a whole, consistent with a normal probability distribution).

In the first assessment the results from the six manual methods, the two 3d Pitots, two S type Pitots, L type Pitot and the vane anemometer, were assessed. This addressed the methods which are all considered as comparable implementations of the manual method which provide point velocity measurements.

The ISO EN 20988 analysis gave the following results. The standard uncertainty of the result measurement y from the application of a manual flow measurement techniques in the range 17.8 m/s to 21.2 m/s, is $u(y) = 0.49$ m/s. The expanded 95 % of result of measurement y using a manual flow measurement method in the range 17.8 m/s to 21.2 m/s is $U_{0.95}(y) = 0.98$ m/s.

Figure 24 provides a plot of the 95% margin of uncertainty about the reference data

$y_R(j)$. The 95% margin of uncertainty $[y_R - U_{0.95}(y); y_R + U_{0.95}(y)]$ is found to encompass $p=97.5$ % of the evaluated 62 measurement results $y(k,j)$. Therefore, the expanded uncertainty $U_{0.95}(y) = 0.98$ m/s is considered to be a well founded measure of the uncertainty.

The uncertainties determined are therefore applicable to the measurement of average flow for an emissions duct in m/s formed by taking a grid of samples of point flow measurements.

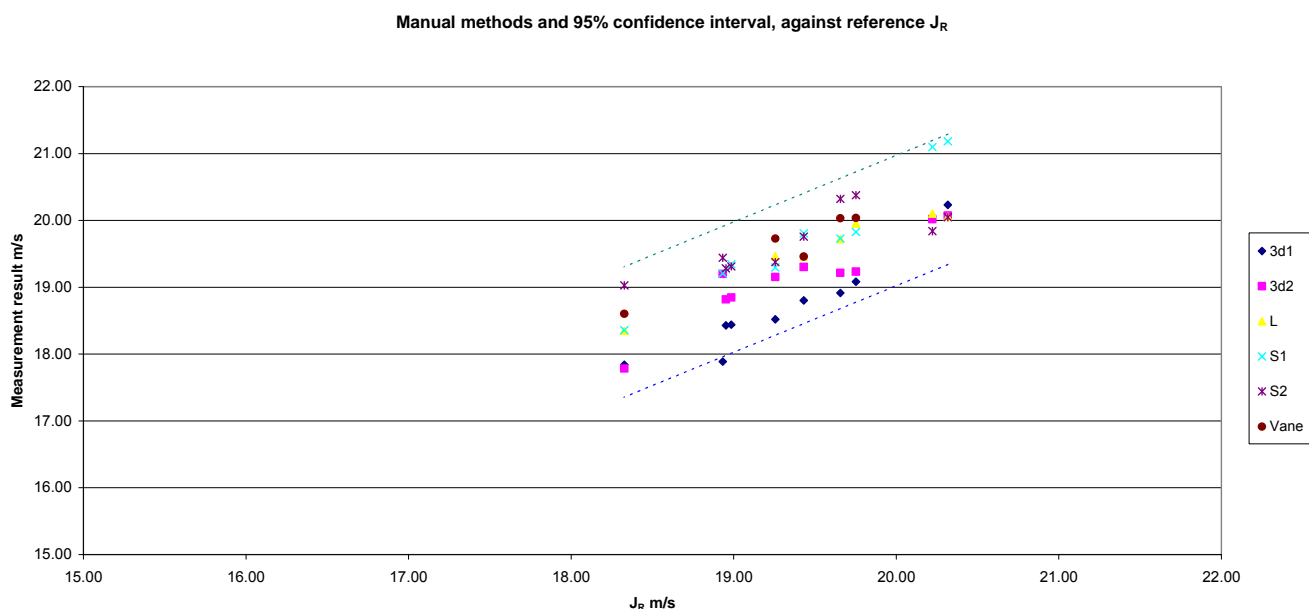


Figure 24 Plot of 95% confidence interval about measurement results for manual flow methods.

A similar uncertainty assessment was carried out to include all of the periodic measurement technique results reported in Table 13, i.e. including the results of the tracer techniques. These assessments were carried out using the ISO EN 20988 assessment approach as described above. Figure 25 presents a plot of the results for the assessment of the ensemble of all periodic methods,

showing the 95% confidence interval. Table 15 presents a summary of the set of ISO EN 20988 uncertainty assessments.

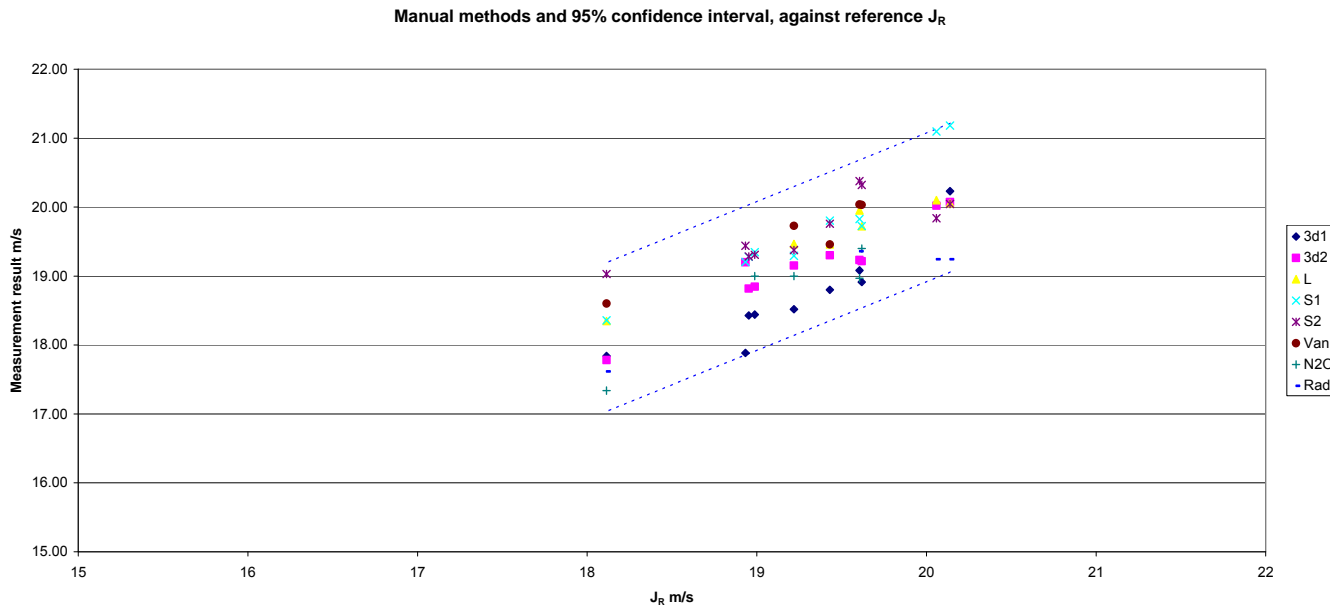


Figure 25 Plot of 95% confidence interval about measurement results for all periodic flow methods

Summary of uncertainty results		
Manual methods (3d, L type, S type, vane anemometer)		
Bias	u_B	0.32 m/s
Standard uncertainty	$u(j)$	0.49 m/s
Expanded uncertainty	$U_{0.95}$	0.98 m/s
All periodic methods (3d, L Type, S Type, vane anemometer, tracer techniques)		
Bias	u_B	0.39 m/s
Standard uncertainty	$u(j)$	0.51 m/s
Expanded uncertainty	$U_{0.95}$	1.08 m/s
Differential pressure methods (3d, L Type, S Type)		
Bias	u_B	0.35 m/s
Standard uncertainty	$u(j)$	0.50 m/s
Expanded uncertainty	$U_{0.95}$	1.00 m/s

Table 14 Uncertainty evaluation of the Manual flow methods

For the tracer techniques only a limited number of repeat measurements coincident with the other manual method measurement periods were available. There were not enough parallel measurements between the tracers to enable a comparison, and no parallel data within the tracer methods. In order to assess the variability of the radioactive transit time tracer method, paired data was assessed between the radioactive transit time tracer method and the UCD1 (60m) AMS. This assessment includes uncertainty components from both the transit time tracer method and the AMS, so it does not give a true indication of the transit time method performance. However, it does provide some information on the repeatability uncertainty of the data used to provide a calibration between these two methods. The EN 14181 Method A linear regression calibration function for the UCD1 (60m) calibrated using the transit time method gave a slope of 0.95, with an intercept of – 0.27 m/s. The regressions statistics gave an R² value of 0.99, indicating the method has a good degree of linearity.

7.4.2 Assessment of calibration of AMS instruments

Calibration functions were determined from the parallel data sets using the manual methods. The calibration functions were determined using the procedures defined in EN 14181. This method allows for two approaches – depending on whether the range of conditions during the calibration determination are significant compared to the range of operation of the instrument, usually defined in terms related to the Emission Limit Value (ELV). However, for flow measurements no ELVs are defined, as flow itself is not a regulated parameter. Typically, for a given site, the flow rate will also remain within a fairly small range – unless there are plant disruptions, or during start-up and shut-down operation. The maximum flow observed during the tests was therefore used as a surrogate ELV in order to assess the spread of data. EN 14181 then allows one of two procedures to be followed, depending on whether the spread of data measured by the SRM is greater (Method A) or less (Method B) than 15% of the ELV. In effect, Method A is a classical least squares linear regression, and Method B is a linear regression constrained to pass through zero. In all cases the spread of data was less than 15% of the maximum value observed during the tests and so Method B is considered as the preferred method. However, in the interest of completeness Method A has also been applied. It is arguable that this may be more appropriate, if for a given calibration application, the AMS is always going to be used within the range of the calibration. However, as will be seen, the small spread of data does give rise to what appear, in certain cases to be, unrealistic calibration functions.

The full EN 14181 approach requires that the zero reading of the AMS be assessed if method B is to be used, generally this is done during functional tests. However, a full functional test and EN 14181 implementation was not carried out during the field validation studies. During the laboratory tests, however, the AMSs available for those tests were checked for zero reading. The results of those tests are given in Table 15, and as can be seen all the tested AMSs gave zero readings for zero flow.

Date	AMS	Type	recorded value	difference rel. *	AMS range
01/03/2010	SICK	CDUS	0.00 m/s	0.00%	40 m/s
01/03/2010	SICK	CDUS	0.00 m/s	0.00%	40 m/s
02/03/2010	Höntzsch	VS	0.01 m/s	0.03%	40 m/s
03/03/2010	FCI	TMF	0.01 m/s	0.03%	40 m/s
03/03/2010	FCI	TMF	0.00 m/s	0.00%	40 m/s
04/03/2010	ABB	DP	0.00 m/s	0.00%	30 m/s
05/03/2010	Höntzsch	Vane	0.00 m/s	0.00%	40 m/s
05/03/2010	SICK	SPUS	-0.01 m/s	-0.03%	40 m/s
08/03/2010	Höntzsch	VS	0.01 m/s	0.03%	40 m/s

Table 15 AMS Zero readings

The EN14181 calibration approach was applied using the L type Pitot results (Table 8), to the each of the AMSs that were installed during the parallel test phase. This did not include the averaging pitot technique, as has been noted earlier this was not installed until later. The QAL2 functions were also determined using the reduced set of data in Table 9, using the L type Pitot. The calibration functions using the Vane and the S type Pitot were also determined. The S type tests had, at most, 10 paired data sets and so do not comply with the EN 14181 requirement for N>15 parallel tests, whereas the L type and vane anemometer calibration data sets both had more than 15 paired data points.

Prior to carrying out the calibration, a Grubbs outlier test was performed on each paired data set. One outlier was determined, for the Ultrasonic cross duct analyser, installed at the 20m sampling location. Test L13 (Table 11) was indicated as an outlier and was removed from the calibration determination for the UCD2. The removal of this outlier made insignificant difference to the calibration function determined by Method B. As has already been mentioned, a further test, made at the 60m level using the L Pitot was also removed (test number 18).

The following describes the EN 14181 procedure followed, using as an example, the data for the L Type calibrating the Ultrasonic Cross Duct analyser at 60m (UCD1 60m).

The input data is given in Table 11.

The difference between the maximum and minimum of the SRM (L type) results was 2.86, and this is less than 15% of the maximum value, and so a Type B analysis is indicated.

There is no zero offset assigned to the AMS readings, and so the Z term in EN 14181 is 0.

EN 14181 Section 6.4 identifies the calibration function as:

$$y_i = a + bx_i + \varepsilon_i$$

where x_i is the i^{th} AMS result,

- y_i is the i^{th} SRM [in this case candidate SRM – L Type Pitot] result
- ε_i is the deviation between y_i and the expected value
- a is the intercept of the calibration function
- b is the slope of the calibration function.

The calibration functions derived for Method A and Method B are :

Method A : $y = 1.05 x - 1.66$

Method B : $y = 0.96 x$

Figures 26 and 27 present the linear fits in a graphical form.

From these results EN 14181 requires a test of the variability. EN 14181 defines a variability measure, S_D and a test criterion derived from the ELV and the 95% uncertainty requirements from the Directive related to the ELV. For flow monitoring neither of these input quantities are defined. For the purposes of this analysis the variability has been calculated and has been reported. For illustrative purposes, a test criterion based on an assumed ELV of 21 m/s (maximum test value) and a target uncertainty of 3% has been used which gives a test criterion of 0.32 m/s.

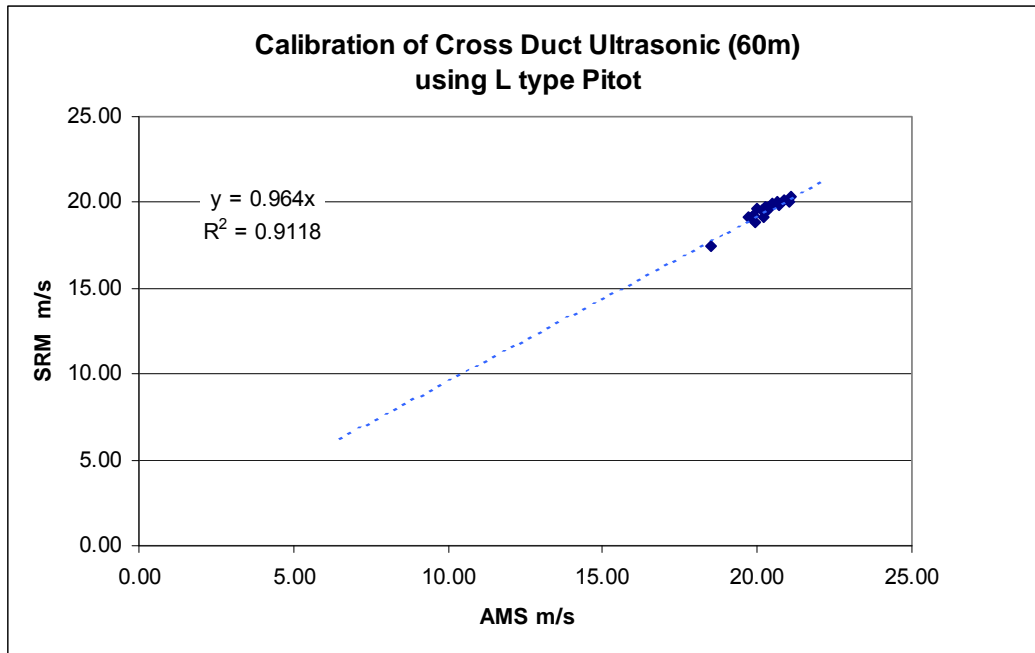


Figure 26 Graphical representation of En 14181 Method B calibration procedure L Type Pitot calibration of Cross Duct Ultrasonic analyser (60m)

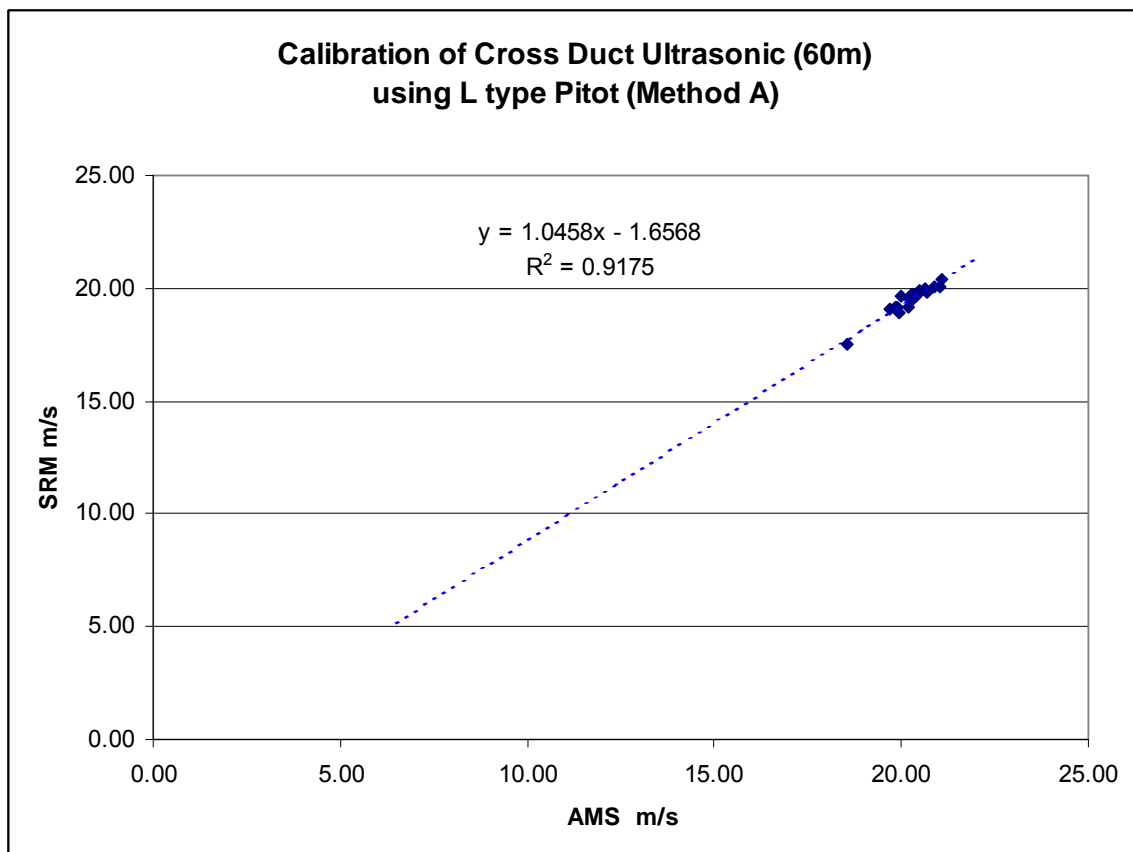


Figure 27 Graphical representation of En 14181 Method A calibration procedure L Type Pitot calibration of Cross Duct Ultrasonic analyser (60m)

Table 16 presents a summary of the calibration results for all the AMSs calibrated using the L type Pitot. As can be seen, two of the AMS have significantly poorer calibration variability, and also generated calibration functions using the Method A approach with very large intercepts. Both these instruments were single point velocity measurement devices, installed at the 60m sampling location. The vortex instrument located at Port 8 was also at the 60m elevation, however, this had a

calibration function that appears to be more acceptable. This is may be because it was on an axis of the sampling location which had a broadly symmetrical flow profile compared to Port 8. This illustrates the importance of characterising the flow profile at any location at which AMS instruments are to be located, and selecting locations which have stable flow profiles. For comparison the calibration functions were also determined using the seven L type data points from Table 9, and the results of this analysis are given in Table 17. As can be seen the Method B approach gives similar results for these reduced data sets, for those calibration functions that passed the variability tests.

EN 14181 Calibration														
QAL2 function against L type														
Reference method: L Type 21 Parallel measurements			Cal (Method B)				Var test < 0.32m/s		Cal (Method A)				Var test < 0.32m/s	
Method A or B		Outlier	a	b	R ²	S _D	Pass	a	b	R ²	Pass	Pass		
Ultrasonic Cross Duct (60m)	B	No	0.00	0.96	0.91	0.18	Y	-1.66	1.05	0.92	0.17	Y		
Ultrasonic Cross Duct (20m)	B	Yes (L13)	0.00	1.17	0.85	0.16	Y	1.54	1.08	0.86	0.15	Y		
Ultrasonic Probe	B	No	0.00	1.09	0.91	0.18	Y	-0.74	1.13	0.91	0.18	Y		
Vortex Port 5	B	No	0.00	1.13	-8.76	1.87	F	15.58	0.23	0.61	0.37	F		
Vortex Port 8	B	No	0.00	0.92	0.91	0.18	Y	-1.15	0.97	0.91	0.18	Y		
Vane	B	No	0.00	0.99	-2.81	1.16	F	15.02	0.23	0.28	0.50	F		
Averaging Pitot			not done											

Table 16 Results of calibration using L Type Pitot

QAL2 function against L type														
7 Tests			Cal (Method B)				Var test < 0.32m/s		Cal (Method A)				Var test < 0.32m/s	
Method A c		Outlier	a	b	R ²	S _D	Pass	a	b	R ²	S _D	Pass		
Ultrasonic Cross Duct (60m)	B	N	0.00	0.96	0.96	0.12	Y	-0.84	1.00	0.96	0.12	Y		
Ultrasonic Cross Duct (20m)	B	N	0.00	1.17	0.96	0.12	Y	0.74	1.12	0.96	0.12	Y		
Ultrasonic Probe	B	N	0.00	1.08	0.97	0.10	Y	-0.50	1.11	0.97	0.10	Y		
Vortex Port 5	B	N	0.00	1.09	-4.03	1.37	F	13.73	0.33	0.91	0.19	Y		
Vortex Port 8	B	N	0.00	0.92	0.95	0.13	Y	-0.43	0.94	0.95	0.13	Y		
Vane	B	N	0.00	0.96	-0.60	0.77	F	11.43	0.40	0.63	0.37	F		
Averaging Pitot														

Table 17 Results of calibration of AMSs using L Type data, 7 points from Table 3

Examples of the calibration functions derived using the Vane anemometer and one of the S type Pitots are given in the following two tables. As can be seen the Method B calibration functions are similar to the L type.

Vane		UCD1	UCD2	Vane	USP	VOR5	VOR8
Method A	b	1.07	1.22	0.28	1.17	0.24	1.02
	a	-2.01	-0.67	14.22	-1.30	15.61	-1.91
Method B	b	0.97	1.17	0.99	1.09	1.13	0.92
	a	0	0	0	0	0	0

Table 18 EN 14181 calibration curves for AMS calibrated using the vane anemometer

S1		VCD(60m)	VCD2 20m	VUSP	VVOR5	VVOR8	VVAN
Method A	b	1.57	1.78	1.73	0.56	1.50	0.80
	a	-12.17	-9.99	-11.31	9.77	-12.18	3.70
Method B	b	0.97	1.18	1.10	1.11	0.93	0.98
	a	0.00	0.00	0.00	0.00	0.00	0.00

Table 19 EN 14181 calibration curves for AMS calibrated using an S Type Pitot (S1)

Table 20 presents a comparison of the EN 14181 Method B calibration function derived for all AMS using each of the manual methods. In each case the largest number of available parallel data points has been used to determine the calibration function. In addition, for comparison, the reduced

number of data points corresponding to the test periods in Table 9 have also been used where these are different. It can be seen that there appear to be systematic differences between the L type, S type and Vane anemometer calibration functions and the 3d and tracer methods. If we assume that an estimate of the influence of the repeatability of the methods during a calibration can be determined from $SD/(\sqrt{N})$ where N is the number of paired data points used to determine the calibration function, then these data can be compared to the variability seen between the calibration functions. This shows that, by this simplified analysis, the repeatability of the methods does not account fully for the variability seen between the calibration functions using different manual methods to calibrate the same AMS. The 3d Pitot flow data were determined using the calibration function from the 'ES' calibration (see Laboratory validation study for comparisons of the two 3d Pitot calibrations). It is believed that this calibration function was determined in a smaller duct than the 'AP' calibration function. It is possible that the 'AP' calibration function may therefore be more appropriate for use in a large duct. The impact of changing to the AP calibration function will be investigated.

An analysis using the ANOVA approach has been undertaken, however the small number of repeat calibrations does not allow a conclusive assessment.

The implementation of the transit time tracer method by Indmeas has an accreditation which gives a traceable calibration with an uncertainty of $\sim 0.5\%$ for the calibration of the UCD1. A further investigation of the apparent systematic variation between the methods will be undertaken in order to inform the standardisation process, of for example the parameters which need to be controlled to minimise systematic sources of uncertainty.

Comparison of EN 14181 Method B calibration functions (slope)						
Manual method	AMS					
	UCD1 (60m)	UCD2 (20m)	USP	VOR5	VOR8	VAN
L	0.96	1.17	1.09	1.13	0.92	0.99
S1	0.97	1.18	1.10	1.11	0.93	0.98
S2	0.97	1.18	1.10	1.11	0.92	0.98
3D1	0.93	1.13	1.05	1.06	0.88	0.94
3D2	0.94	1.15	1.07	1.08	0.90	0.95
Vane	0.97	1.18	1.10	1.17	0.93	1.02
Tracer dilution	0.93	1.13	1.05	1.10	0.89	0.95
Tracer Transit time	0.94	1.15				
L reduced ³	0.96	1.17	1.08	1.09	0.92	0.96
V reduced ³	0.97	1.18	1.10	1.14	0.92	0.99
Tracer Transit time (reduced) ³	0.92	1.12	1.04	1.05	0.88	0.91

Table 20 Comparison of Calibration functions derived from all manual methods

Notes

1) L type and Vane calibration functions have been determined from the full data sets as defined in Table 14

2) The radioactive tracer calibration functions were derived from all of the reported tracer data, (plotted in Figure 5). Data was only available over coincident time periods for the UCD1 and UCD2 AMSs.

3) The calibration functions labelled 'reduced' have been derived from the smaller number of data sets which are from coincident sampling periods as defined in Table 15.

7.4.3 Assessment of AMS performance

In order to assess the AMS performance, data from a period after the parallel manual method testing period has been analysed. During this period the ABB Torbar averaging Pitot was also installed.

In order to assess the variability of the AMSs, it is necessary to remove Bias terms. In order to do this, the AMSs were calibrated against the ultrasonic cross duct analyser installed at 60m, which had been calibrated using the radioisotope time of flight tracer method, using a Method B calibration function. This calibration function gave a calibration factor of 0.94 (as reported in Table 20). Therefore, the UCD 60 was used in effect used as a calibration transfer. It is important to note that for this assessment the absolute calibration (by the tracer method) is not being assessed – as any uncertainty in this calibration stage will be transferred to all the other AMSs as a common bias, which will not be quantified by the repeatability assessment. In addition, because all the data points are used to derive the regression curves used to normalise the data between the UCD60 and the other AMSs, these regression fits remove any bias between the AMSs. This approach therefore allows an assessment of the pooled standard deviation following this calibration, which gives an indication of the repeatability or random variation between the AMS, over a relatively short time period. It does not assess biases, or longer time period variability, such as drift. Figure 28 shows the AMSs plotted against the UCD60 calibrated data and presents the regression analyses.

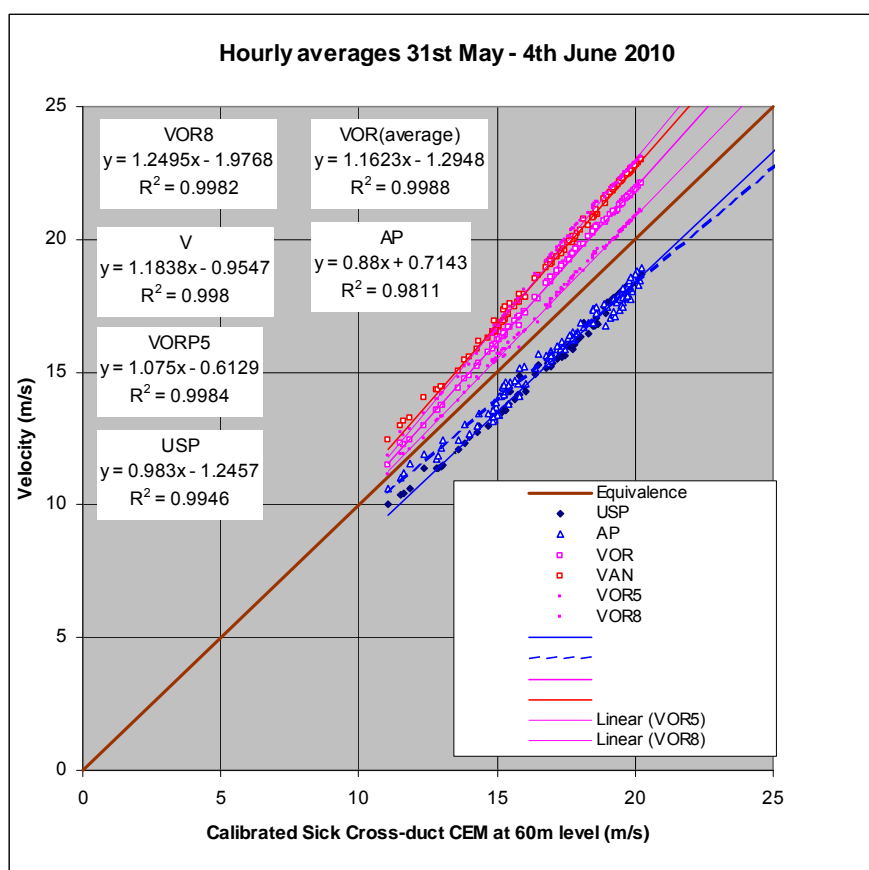


Figure 28 Calibration curves for all AMSs against calibrated UCD60

As can be seen, the AMSs appear to be quite linear over the range of measurements. It should also be noted that this calibration has been done by plotting the AMSs against the UCD1 (60m), deriving the linear calibration function, and then inverting it. (See the note on EN14181 calibration approach above). Figure 29 shows the time series of AMS data used for this assessment, the differences

between the plots gives an indication of the spread of the AMS data before any calibration has been applied. The UCD2 (20m) data were not available in time for this assessment.

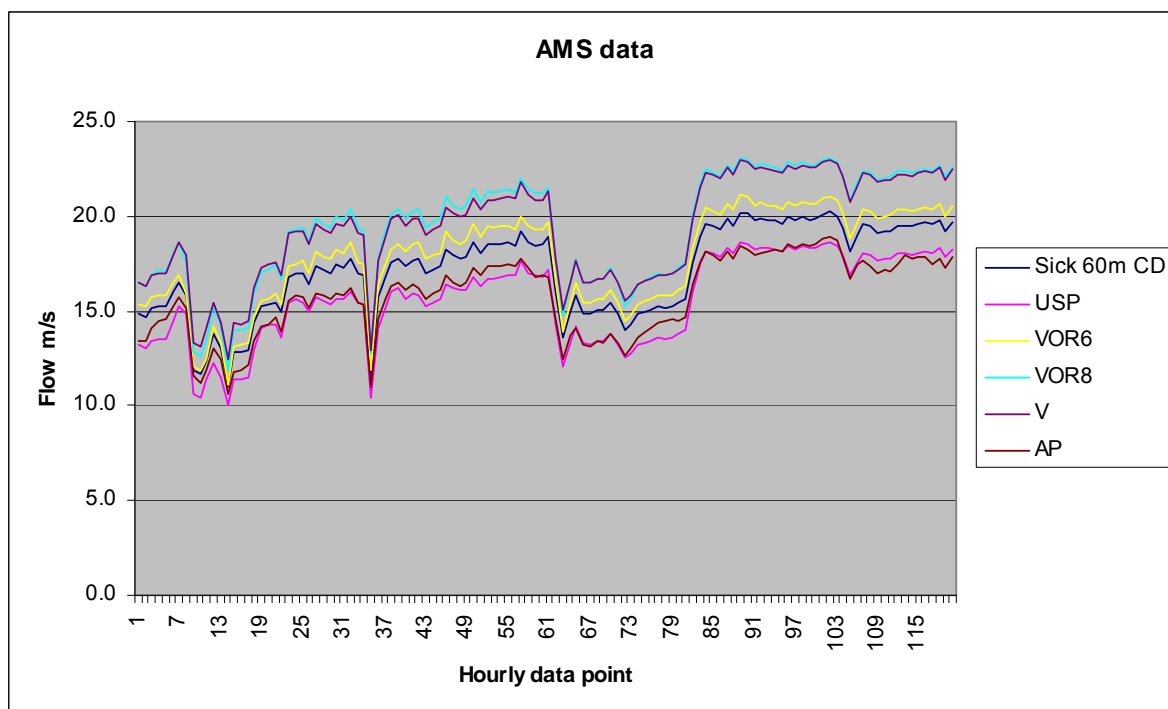


Figure 29 Time series of AMS data used for assessment

After applying the calibration curves illustrated in Figure 28, the systematic differences between the data are minimised. This allows an assessment of the repeatability of the AMS methods to be made by calculating both the field variability Var_f (based on R_f as defined in EN 15267-3) and pooled standard deviations. Note Var_f has been determined from paired data using a calculation based on that for Reproducibility as defined in EN 15267-3. However as the validation study is not a performance test and did not use paired instruments, the calculation has been used to give an indication of the variability of the methods and is not a strict application of Reproducibility as defined in EN 15267-3. The time series of calibrated data is shown in Figure 30. The closeness of fit between the data is due to the regression being performed over the whole data set, and does not provide any indication of the 'quality' of the calibration itself, it mainly indicates that the different AMSs do not exhibit significant nonlinear behaviour over the range of the measurements.

Table 21 presents the variability (Var_f) and pooled standard deviation analyses for the AMSs. The repeatability uncertainty U_{rep} has been calculate using a coverage factor of $k=1.96$, as the number of data points used in this assessment is 120.

	USP	VOR5	VOR8	V	AP
	m/s	m/s	m/s	m/s	m/s
Pooled stdv	0.12	0.07	0.07	0.07	0.23
$U_{rep} (k=1.96)$	0.24	0.13	0.14	0.14	0.45
Var_f	0.24	0.13	0.14	0.14	0.45

Table 21 Field repeatability and variability for AMS

A further analysis was carried out to assess the uncertainty in the field including the effect of the calibration using a manual method, reported in Table 22. To assess this the individual calibration functions (determined using EN 14181 Method B) derived for each AMS were applied to the AMS

data assessed in this period. No calibration function was available for the averaging Pitot (AP), as this was not present during the parallel measurements with the manual methods.. This instrument was therefore left 'uncalibrated'. Data were also not available at the time of this assessment for the UCD2 (20m). The assessment was made using the average value for all the calibrated AMS data as the reference value. It is not surprising that the AMSs for which the L-Type calibration functions gave a poorer fit (See Table 19), have reproducibility and field repeatability figures that are worse. This is because the calibration function will affect these performance metrics (ie if the calibration introduces a bias into the data this will have an influence on the repeatability and variability statistics). Similarly for the AP the results include an effect of the bias due to the lack of calibration for this AMS, so the figures for this AMS do not give a representation of the repeatability performance of this AMS. This provides further confirmation that it is important to select good sample locations for both the AMS and the reference method, at which a representative calibration can be made. It also shows the importance of testing paired instruments in the field as a part of EN15267 performance evaluation, as this will enable a measure of the repeatability and reproducibility of the AMS to be determined during performance evaluation for instrument certification to EN 15267-3.

	UCD1	USP	VOR5	VOR8	V	AP
	m/s	m/s	m/s	m/s	m/s	m/s
Pooled stdv	0.55	0.95	1.23	0.33	0.57	1.84
$U_{rep} (k=1.96)$	1.07	1.86	2.41	0.64	1.11	3.60
Rf	1.09	1.87	2.44	0.65	1.12	3.64

Table 22 Field repeatability and variability, for calibration using L Type Pitot

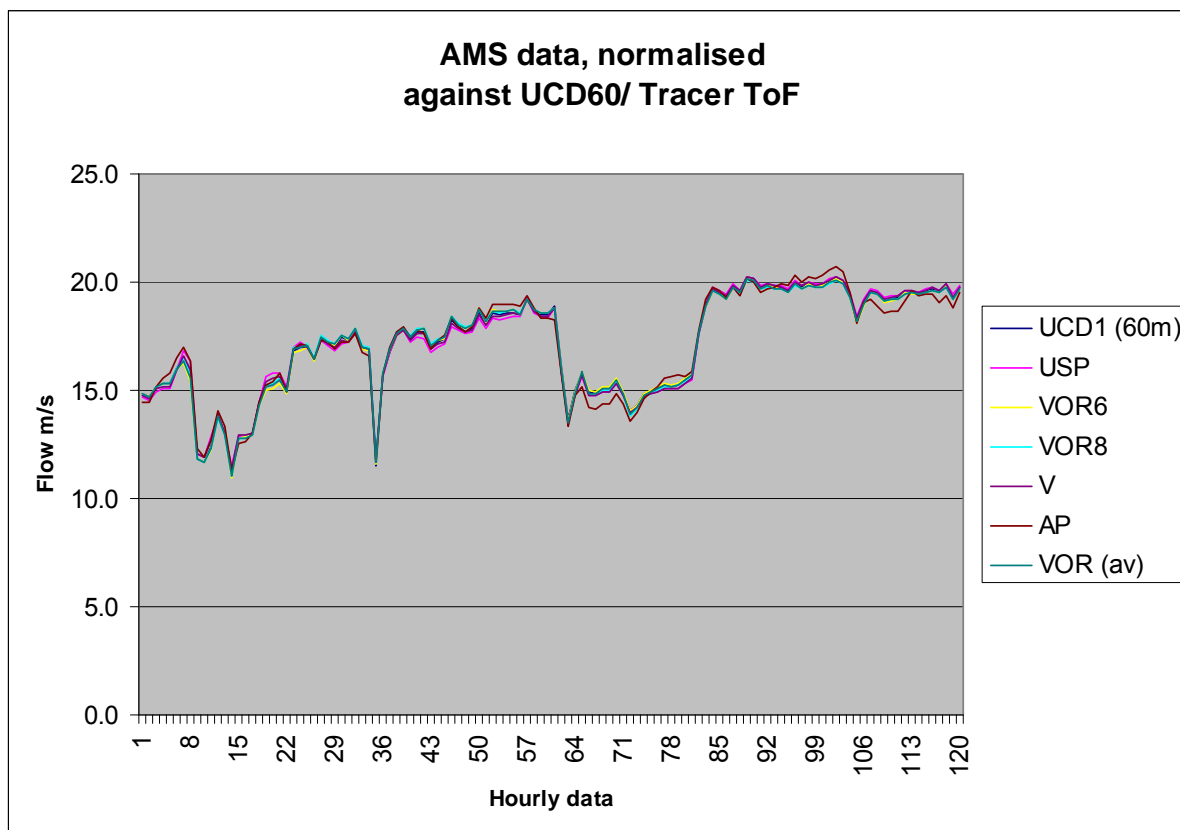


Figure 30 Time series of AMS data, after normalisation

7.5 Performance evaluation of field test 2, 'Wilhelmshaven'

A full description of the field tests, including description of the test site, and the experimental design, and data analysis, is given in the field test report "CEN Working Group 23: Stack Gas Velocity Standards Second validation field trial: Wilhelmshaven (coal fired power plant)" produced by E.ON New Build & Technology (subsequently referred to herein as the 'second field validation study report').

In the second field validation study, the L type, 3d and S type Pitots were assessed, together with a 2G Pitots. The manual vane anemometer was not available in the second field validation study. The tracer techniques did not provide data. No authorisation was available to use the radioactive transit time technique. The dilution tracer technique was attempted to be used, but it was not possible to achieve suitable mixing of the entrained tracer in the stack flow. Single installations of the ultrasonic cross duct analyser, thermal mass flux, vane and vortex instruments were deployed, with an additional AMS, the correlation technique, being installed for part of the tests. The vane and vortex instruments were only installed for a short period and could not be assessed statistically.

As described in the field test report, the tests at Wilhelmshaven were interrupted by a plant shutdown. As can be seen from the summary of the test periods, given in Table 23, the shutdown occurred during T6, invalidating this test. Following this, due to logistical issues, only the 3d and L type Pitots were operated in a parallel mode. The vane anemometer was not re-installed, and so for this study the vane anemometer can be effectively excluded. In addition the S type was not performed in parallel with the other manual methods, and the 2G Pitot was only run in parallel for tests T10 to T 14, which is unfortunate as this method was not available for Field Study 1. The AMS data has been averaged over the test periods, in the same way as for Field Study 1.

During this validation study, however, the L type Pitots were run in parallel, with both pitots sampling the same area of the stack at the same time. This provides a set of data which can be used to determine repeatability. It was not possible to do this with the 3d pitots. It was attempted with the S type Pitot, however, there was apparently some interference observed during T1 between the two Pitots (See the Field test report) and so they were separated for subsequent tests..

Traverse	3D & L type			S type (no C/L)			2G type			Vane		
	Date	Start	End	Date	Start	End	Date	Start	End	Date	Start	End
T1	06-Jul-10	11:30:00	14:42:00	06-Jul-10	11:30:35	14:41:42	-	-	-			
T2	06-Jul-10	15:52:00	17:10:00	06-Jul-10	15:52:00	17:09:30	06-Jul-10	15:52:00	17:09:30			
T5	07-Jul-10	09:18:00	10:49:00	07-Jul-10	09:18:30	10:48:30	07-Jul-10	09:18:30	10:48:30	07-Jul-10	09:18:00	10:49:00
T6 (part)	07-Jul-10	11:17:00	11:27:00	07-Jul-10	11:17:00	11:27:00	07-Jul-10	11:17:00	11:27:00	07-Jul-10	11:17:00	11:27:00
T7	20-Jul-10	10:23:00	11:41:00	22-Jul-10	09:27:00	10:31:00	21-Jul-10	12:08:00	13:18			
T8	20-Jul-10	13:18:00	14:49:00	22-Jul-10	10:33:00	12:06:00	20-Jul-10	15:54:00	16:36			
T9	20-Jul-10	15:02:00	16:09:00	22-Jul-10	13:17:00	14:21:00	21-Jul-10	12:16:00	13:18			
T10	20-Jul-10	16:43:00	17:42:00	22-Jul-10	14:23:00	15:23:00	20-Jul-10	16:43:00	17:42:00			
T11	21-Jul-10	09:14:00	10:17:00	22-Jul-10	15:25:00	16:25:00	21-Jul-10	09:14:00	10:17:00			
T12	21-Jul-10	10:53:00	11:52:00	22-Jul-10	16:27:00	17:25:00	21-Jul-10	10:53:00	11:52:00			
T13	21-Jul-10	13:33:00	14:34:00	23-Jul-10	08:31:00	09:39:00	21-Jul-10	13:33:00	14:34:00			
T14	21-Jul-10	14:47:00	15:50:00	23-Jul-10	09:41:00	10:43:00	21-Jul-10	14:47:00	15:50:00			
N _{traverse}		11			11			10			1	

Table 23 Summary of test times for Wilhelmshaven

Tables 24 and 25 present summaries of the average velocity measurements determined over the parallel test periods, for the manual and AMS methods respectively. Results are also given for the flow determined by calculation (labelled 'process calculation'), as described in the field test report, and in accordance with the methods being standardised by WG23. The results in the table are representative of the periods when multiple techniques were deployed. There were in some cases slight differences in the actual time periods of sampling for the different methods which are marked as being nominally coincident. The statistical analysis has been carried out using CEM data averaged over the actual recorded periods for each manual method. For simplicity all of those data are not reported here. For example, for periods marked as being coincidental for the L-type, S-type, 3d and 2G Pitots, the actual time periods over which these different Pitots measured the flow are slightly different, and separate averages for the AMS data were calculated corresponding to the actual time periods. For simplicity Table 25 only reports the average AMS data corresponding to the L-type Pitot measurement periods.

Test No	Filed Test ID	Date	Period of test	Manual Method Results									
				3d1	3d2	L1	L2	S1	S2	2G1	2G2		
				m/s	m/s	m/s	m/s	m/s	m/s	m/s	m/s		
L1	T1	L,3d,S	06-Jul	11:30	14:42	27.64	27.92	28.31	28.31	29.67	29.43		
L2	T2	L,3d,S,2G	06-Jul	15:52	17:10	23.71	24.97	23.78	23.76	24.17	21.76	22.07	24.37
L3	T5	L,3d,S,2G	07-Jul	09:18	10:49	29.30	30.57	30.37	30.57	31.52	31.10	28.39	28.89
L4	T7	L,3d	20-Jul	10:23	11:41	22.79	22.61	23.57	23.55				
L5	T8	L,3d	20-Jul	13:18	14:49	22.86	24.10	23.74	23.75				
L6	T9	L,3d	20-Jul	15:02	16:09	23.18	24.07	23.57	23.45				
L7	T10	L,3d,2G	20-Jul	16:43	17:42	23.07	24.05	23.68	23.53			25.49	25.42
L8	T11	L,3d,2G	21-Jul	09:14	17:42	28.00	29.08	28.87	28.80			30.04	31.39
L9	T12	L,3d,2G	21-Jul	10:53	11:52	26.65	26.82	27.07	27.00			28.67	30.23
L10	T13	L,3d,2G	21-Jul	13:33	14:34	23.87	24.24	23.92	23.67			25.10	26.04
L11	T14	L,3d,2G	21-Jul	14:47	15:50	23.61	23.96	24.07	23.96			24.98	26.70
L12	T7'	S	22-Jul	09:27	10:31					29.25	28.75		
L13	T8'	S	22-Jul	10:33	12:06					29.21	28.90		
L14	T9'	S	22-Jul	13:17	14:21					26.29	25.99		
L15	T10'	S	22-Jul	14:23	15:23					25.93	25.48		
L16	T11'	S	22-Jul	15:25	16:25					25.08	24.66		
L17	T12'	S	22-Jul	16:27	17:25					24.77	24.97		
L18	T13'	S	23-Jul	08:31	09:39					27.63	27.13		
L19	T14'	S	23-Jul	09:41	10:43					27.97	27.53		
L20	T7''	2G	21-Jul	12:08	13:18							24.83	26.62
L21	T8''	2G	20-Jul	15:54	16:36							23.55	26.20
L22	T9''	2G	21-Jul	12:16	13:18							23.63	25.89

Table 24 Summary of manual method results from the second field validation study

Test No	Filed Test ID	Date	Period of test	Process Calculation	AMS Results						
					TMF	VAN	VOR	UCD	COR		
					m/s	m/s	m/s	m/s	m/s		
L1	T1	L,3d,S	06-Jul	11:30	14:42	28.15	24.20	31.74	28.44	28.88	
L2	T2	L,3d,S,2G	06-Jul	15:52	17:10	24.07		27.09	23.28	24.65	
L3	T5	L,3d,S,2G	07-Jul	09:18	10:49	29.76		33.61	30.29	30.69	
L4	T7	L,3d	20-Jul	10:23	11:41	23.15	19.39			24.35	24.76
L5	T8	L,3d	20-Jul	13:18	14:49	23.56	19.16			24.40	25.08
L6	T9	L,3d	20-Jul	15:02	16:09	23.60	18.99			24.51	25.16
L7	T10	L,3d,2G	20-Jul	16:43	17:42	23.54	18.79			24.47	25.09
L8	T11	L,3d,2G	21-Jul	09:14	17:42	28.80	22.95			29.56	31.19
L9	T12	L,3d,2G	21-Jul	10:53	11:52	27.37	21.67			27.99	29.57
L10	T13	L,3d,2G	21-Jul	13:33	14:34	23.96	18.42			24.79	25.36
L11	T14	L,3d,2G	21-Jul	14:47	15:50	23.83	18.32			24.73	25.27
L12	T7'	S	22-Jul	09:27	10:31	27.90	21.59			29.08	30.20
L13	T8'	S	22-Jul	10:33	12:06	28.22	21.90			29.29	30.46
L14	T9'	S	22-Jul	13:17	14:21	25.38	19.91			26.07	27.13
L15	T10'	S	22-Jul	14:23	15:23	24.82				25.58	26.53
L16	T11'	S	22-Jul	15:25	16:25	24.01				24.80	25.49
L17	T12'	S	22-Jul	16:27	17:25	24.08				24.87	25.64
L18	T13'	S	23-Jul	08:31	09:39	26.39				27.27	28.36
L19	T14'	S	23-Jul	09:41	10:43	26.64				27.55	28.79
L20	T7''	2G	21-Jul	12:08	13:18	24.01	18.65			24.65	25.58
L21	T8''	2G	20-Jul	15:54	16:36	23.56	18.94			24.61	25.12
L22	T9''	2G	21-Jul	12:16	13:18	24.21	18.45			24.53	25.39

Table 25 Summary of AMS results averaged over the test periods for the second field validation study

7.5.1 Repeatability and uncertainty of manual methods in the second field validation study.

During the second field validation study, as has been described above, there were a number of different periods of measurement, and therefore it was not possible to form ensemble performance statistics for all the different methods deployed. However, paired sets of measurements were carried out for each Pitot type which was used. In addition, the 2G Pitot was used during the second validation study, which had not been available during the first study. This Pitot is described in the validation study report, in overview, it is a 2 axis Pitot (i.e. it simultaneously measures differential pressure on two orthogonal axes), designed to meet the requirements of the EPA Method 2G (hence the name).

The paired data from each Pitot method were analysed using the same methodology as described for the first field validation study, to provide pooled standard deviations for the methods, reported in Table 26. As can be seen, L type Pitots gave very good repeatability performance. Because these Pitots were mechanically linked together, this uncertainty analysis is not affected by differences caused by any inhomogeneity in the flow profile or other parameters (e.g. gas density).

The variability (Var_f) for the paired methods was determined in accordance with the procedures given for R_f in EN 15267-3. These data are reported in Table 27. Note Var_f has been determined from paired data using a calculation based on that for Reproducibility as defined in EN 15267-3. However as the validation study is not a performance test and did not use paired instruments, the calculation has been used to give an indication of the variability of the methods and is not a strict application of Reproducibility as defined in EN 15267-3.

Before determining these results the paired data sets were assessed for outliers, by performing the Grubbs Test. Table 28 presents the results of these assessments, two pairs of results were identified as outliers, corresponding to tests T2 and T12. These data were excluded from the statistical analysis. This is acceptable so long as a similar exclusion of outliers is also carried out when the methods are used to determine flow for mass emissions calculations or calibrate AMS.

Pooled standard deviations for paired manual methods			
Paired S Type Pitots		Paired L Type Pitots	
Mean	27.86 m/s	Mean	25.51 m/s
Pooled std ^a	0.29 m/s	Pooled std ^a	0.09 m/s
k	2.11	k	2.08
U(95)	0.60 m/s	U(95)	0.17 m/s
Rel stdv	1.03 %	rel stdv	0.34 %
Urel(95)	2.18 %	Urel(95)	0.70 %
Paired 2G Pitot		Paired 3d Pitots	
Mean	26.43 m/s	Mean	25.32 m/s
Pooled std ^a	1.20 m/s	Pooled std ^a	0.60 m/s
k	2.09	k	2.08
U(95)	2.52 m/s	U(95)	1.26 m/s
Rel stdv	4.55 %	Rel stdv	2.38 %
Urel(95)	9.53 %	Urel(95)	4.96 %

Table 26 Uncertainty in the manual paired manual methods used in second validation study, determined from pooled standard deviation

Reproducibility				
	S Type	L Type	2G	3d
S _D	0.09	0.11	0.85	0.51
K	2.31	2.23	2.26	2.23
Var _f	0.21	0.25	1.90	1.15

Table 27 Variability determined for paired manual methods for the second field validation study

Method	Result of Grubbs outlier test	Identified outliers
L	no outliers	
3d	no outliers	
S	outliers	T2,T12
2G	no outliers	

Table 28 Result of Grubbs outlier test on paired manual method results from second validation study

The uncertainties of the manual methods were also determined from an assessment of the paired data undertaken in accordance with ISO EN 20988 and are reported in Table 29. The experimental design can be considered to match A6 "Paired measurements of two identical measuring systems" as defined in ISO EN 20988. The analysis provides information on the uncertainty due to the bias between the two measurements. The uncertainty procedure then makes use of the relative size of this term u_B compared to the standard uncertainty u , to determine a the method to use to estimate the degrees of freedom, and hence the coverage factor to be used to determine the expanded uncertainty $U_{0.95}$. For the L type Pitot this assessment passed the criterion $u_B^2 \leq 0.5 \cdot u(j)^2$, and the number of degrees of freedom equal to the number of paired tests. The other techniques do not meet this criterion, and for these, Section 7.4 of ISO EN 20988 applies.

In interpreting these uncertainty values, it should be recognised that the uncertainties determined for the S type, 3d and 2G Pitots include the effect of determining the average flow across the duct over the same period, but with the grid of flow measurement being determined in a different order between the pair of methods (i.e. S1 will have sampled the grid over the same period as S2, but they will have sampled different parts of the grid at the same time, whereas L1 and L2 both sampled the same points across the grid at the same time.). The difference between the L Type uncertainties and the other techniques implies there is an effect of the sampling process, and therefore the uncertainties for the S type, 3d and 2G Pitots may be considered more representative of the uncertainty of a single calibration point made when using these methods, and the uncertainty of the L type may be considered representative of the uncertainty of individual point flow measurements, made using these Pitots.

Paired L Type Pitots		
Bias	u_B	0.05 m/s
Standard uncertainty	$u(j)$	0.09 m/s
Expanded uncertainty	$U_{0.95}$	0.19 m/s
Paired S Type Pitots		
Bias	u_B	0.53 m/s
Standard uncertainty	$u(j)$	0.58 m/s
Expanded uncertainty	$U_{0.95}$	1.31 m/s
Paired 3d Pitots		
Bias	u_B	0.70 m/s
Standard uncertainty	$u(j)$	0.60 m/s
Expanded uncertainty	$U_{0.95}$	1.36 m/s
Paired 2G Pitots		
Bias	u_B	1.50 m/s
Standard uncertainty	$u(j)$	1.20 m/s
Expanded uncertainty	$U_{0.95}$	2.72 m/s

Table 29 Uncertainty analysis of paired manual method results from second field validation study

7.5.2 AMS performance in second field validation study

The repeatability performance of the AMSs installed in the second field validation study has been assessed in a similar way to that carried out in the analysis of the first field validation study. However, time series of data were not readily available for the assessment in the same way as for the 'post test period' data used in the analysis of the first field validation study. The assessment was therefore carried out using the mean flow data determined over the test periods as reported in Table 26. The Vortex and Vane AMSs were installed for such a short period that the assessment of these instruments should not be taken as being meaningful. In order to assess the AMS field repeatability and reproducibility bias between the instruments must be removed. This has been achieved by normalising the AMS data against the plant calculated flow data. The calculated flow was determined from process conditions as described in the second field validation test report. Table 31 presents the calibration functions determined for each AMS against the plant-calculated flow. Each AMS data set was normalised using these calibration functions. The repeatability $U_{0.95}$ and variability Var_f for each AMS was then determined, in the same way as described for the first validation study, for the normalised data, using the calculated flow as the reference value. These results are reported in Table 32. It should be noted, as for the analysis of the first field validation study, that the use of the plant flow as a reference was solely done to remove bias between the AMS, and does not ascribe any particular status to the plant calculated data. A further analysis was carried out to determine the repeatability and reproducibility of the AMS data, following calibration against the L type Pitot (the calibration results are described in the following section). For these analyses, the mean of the calibrated AMS results was used as the reference value. These results are presented in Table 33. If the Vane and Vortex data sets are discounted, then it can be seen that the repeatability's and variability's are similar when the influence of the L type pitot calibration are

included, (i.e. by comparing Tables 33 and 34) which implies the calibration does not significantly impact the uncertainties.

	TMF	VAN	VOR	UCD	COR
Slope	1.05	0.87	0.81	0.98	0.85
Intercept	4.16	0.45	5.27	-0.36	2.39
R ²	0.86	1.00	1.00	0.99	1.00

Table 30 Calibration of AMS against plant data

	TMF	VAN	VOR	UCD	COR
U _{0.95}	1.22	0.02	0.08	0.31	0.17
S _D	0.79	0.01	0.06	0.20	0.11
K	2.14	4.30	4.30	2.08	2.10
Var _f	1.70	0.06	0.25	0.41	0.23

Table 31 Repeatability and Variability for AMS Data calibrated against calculated flow

	TMF	VAN	VOR	UCD	COR
U _{0.95}	1.37	0.10	0.93	0.31	0.35
SD	0.88	0.06	0.71	0.20	0.22
K	2.14	4.30	4.30	2.08	2.10
Var _f	1.89	0.24	3.06	0.42	0.47

Table 32 Repeatability and Variability for AMSs calibrated by L Type Pitot (L1) in second field test

7.5.3 EN 14181 calibrations of AMS

Calibration functions were determined in accordance with EN14181 for the AMSs installed during the second field validation study. Each individual manual method was used to calibrate each AMS. In addition calibration functions were also determined for the plant process calculated flow rate determined from process conditions. Calibration functions were derived using EN 14181 Method A and Method B approaches. Method B is the approach that would be required based on the selection procedure in EN 14181. The calibration functions determined for all the AMS methods, calibrated using each of the manual methods, are presented in Table 34.

The Vane and Vortex AMSs were only installed for a short initial period and so the calibration functions for these devices are not representative, and should not be considered as meaningful.

A further series of regression analyses were carried out to assess whether there was any benefit to using any higher order terms in the regression fit. These analyses are summarised in Table 38. It can be seen that there is little benefit to be gained by fitting the data to a second order polynomial,

and in most cases the spread of data is so small that this is more likely to result in over-fitting of the data, with a subsequent loss of quality.

L1	Process Calculation	AMS Results					
		TMF	VAN	VOR	UCD	COR	
Method A	slope	1.02	1.15	1.00	0.93	1.05	0.81
	intercept	-0.40	2.12	-3.45	2.12	-1.95	3.43
	R ²	0.99	0.92	1.00	1.00	1.00	0.99
Method B	slope	1.00	1.26	0.89	1.01	0.97	0.94
	intercept	0.00	0.00	0.00	0.00	0.00	0.00
L2							
Method A	slope	1.05	1.17	1.03	0.95	1.07	0.81
	intercept	-1.11	1.69	-4.26	1.48	-2.70	3.19
	R ²	0.98	0.93	1.00	0.99	0.99	0.99
Method B	slope	1.00	1.25	0.89	1.01	0.97	0.93
	intercept	0.00	0.00	0.00	0.00	0.00	0.00
3d1							
Method A	slope	0.96	1.08	0.85	0.79	0.98	0.79
	intercept	0.60	2.91	0.55	5.28	-0.71	3.50
	R ²	0.99	0.86	1.00	1.00	0.99	0.98
Method B	slope	0.98	1.23	0.87	0.98	0.95	0.92
	intercept	0.00	0.00	0.00	0.00	0.00	0.00
3d2							
Method A	slope	0.99	1.12	0.82	0.75	1.01	0.81
	intercept	0.53	2.85	2.70	7.31	-0.74	3.50
	R ²	0.96	0.83	0.96	0.95	0.95	0.95
Method B	slope	1.01	1.26	0.90	1.02	0.98	0.94
	intercept	0.00	0.00	0.00	0.00	0.00	0.00
S1							
Method A	slope	1.16	1.56	1.13	1.05	1.09	0.90
	intercept	-3.18	-4.82	-6.36	-0.26	-2.17	1.88
	R ²	0.98	0.98	1.00	1.00	0.98	0.99
Method B	slope	1.04	1.34	0.92	1.04	1.01	0.97
	intercept	0.00	0.00	0.00	0.00	0.00	0.00
S2							
Method A	slope	1.24	1.52	1.43	1.33	1.17	0.85
	intercept	-5.76	-4.27	-17.03	-9.28	-4.89	2.99
	R ²	0.89	0.99	1.00	1.00	0.90	1.00
Method B	slope	1.02	1.32	0.87	0.99	0.99	0.96
	intercept	0.00	0.00	0.00	0.00	0.00	0.00
2G1							
Method A	slope	0.91	-0.47	0.97	0.91	0.93	0.92
	intercept	2.78	32.73	-4.07	0.76	1.41	1.32
	R ²	0.72	0.03	1.00	1.00	0.77	0.91
Method B	slope	1.01	1.29	0.83	0.94	0.98	0.97
	intercept	0.00	0.00	0.00	0.00	0.00	0.00
2G1							
Method A	slope	0.05	3.69	0.69	0.65	0.08	-0.28
	intercept	26.26	-39.84	5.71	9.16	25.55	35.49
	R ²	0.00	0.08	1.00	1.00	0.01	0.08
Method B	slope	1.09	1.55	0.88	0.99	1.06	1.05
	intercept	0.00	0.00	0.00	0.00	0.00	0.00

Table 33 EN 14181 calibration functions determined for all AMS in second field study

Manual methods against UCD										
	least squares regression			least squares regression, c=0			quadratic regression, Ax ² +Bx,c=0			number of traverses
	m	c	r ²	m	r ²	A	B	r ²		
2g2	0.805	6.2	0.743	1.041	0.679	-0.009	1.28	0.752	10	
2g1	0.931	1.4	0.772	0.985	0.769	-0.0024	1.05	0.773	10	
3d1	0.99	-1.3	0.986	0.941	0.983	0.0017	0.9	0.986	11	
3d2	1.021	-1.4	0.955	0.968	0.953	0.002	0.91	0.956	11	
l1	1.063	-2.4	0.995	0.973	0.988	0.0032	0.89	0.995	11	
l2	1.09	-3.1	0.992	0.972	0.98	0.0043	0.86	0.992	11	
s1	1.127	-3.1	0.98	1.012	0.97	0.0041	0.9	0.98	11	
s2	1.215	-6	0.902	0.994	0.873	0.0078	0.78	0.901	11	
AMSS vs Plant calculated flow										
	least squares regression			least squares regression, c=0			quadratic regression, Ax ² +Bx,c=0			
	m	c	r ²	m	r ²	A	B	r ²		
TMF	0.798	-0.01	0.858	0.798	0.858	0.0002	0.793	0.858	11	
VAN	1.146	-0.51	1	1.128	1	0.0007	1.107	1	3	
VOR	1.239	-6.51	1	1.002	0.963	0.0091	0.749	0.999	3	
UCD	1.003	0.79	0.994	1.033	0.999	0.0012	1.063	1	19	
COR	1.174	-2.6	0.994	1.072	0.991	0.0039	0.971	0.999	16	
Manual methods comparison between paired data										
	least squares regression			least squares regression, c=0			quadratic regression, Ax ² +Bx,c=0			reproducibility m/s
	m	c	r ²	m	r ²	A	B	r ²		
2g1-2g2	0.832	5.8	0.893	1.056	0.828	-0.008	1.26	0.886	2.7	
3d1-3d2	1.026	0	0.96	1.028	0.96	-0.0001	1.025	0.96	1.3	
l1-l2	1.027	-0.7	0.999	0.998	0.998	0.0011	0.97	0.999	0.2	
s1-s2	1.093	-3.1	0.945	0.998	0.998	0.0011	0.97	0.999	1.3	

Table 34 Summary of regression analyses carried out on data from second field validation study

7.6 Conclusions

The validation studies have provided a valuable set of test data which has been incorporated into the standardization activities being undertaken within WG23. This will enable the development and refinement of the performance characteristics, method performance data and quality control procedures within the standards.